

Nucleosynthesis in Late Stellar Burning

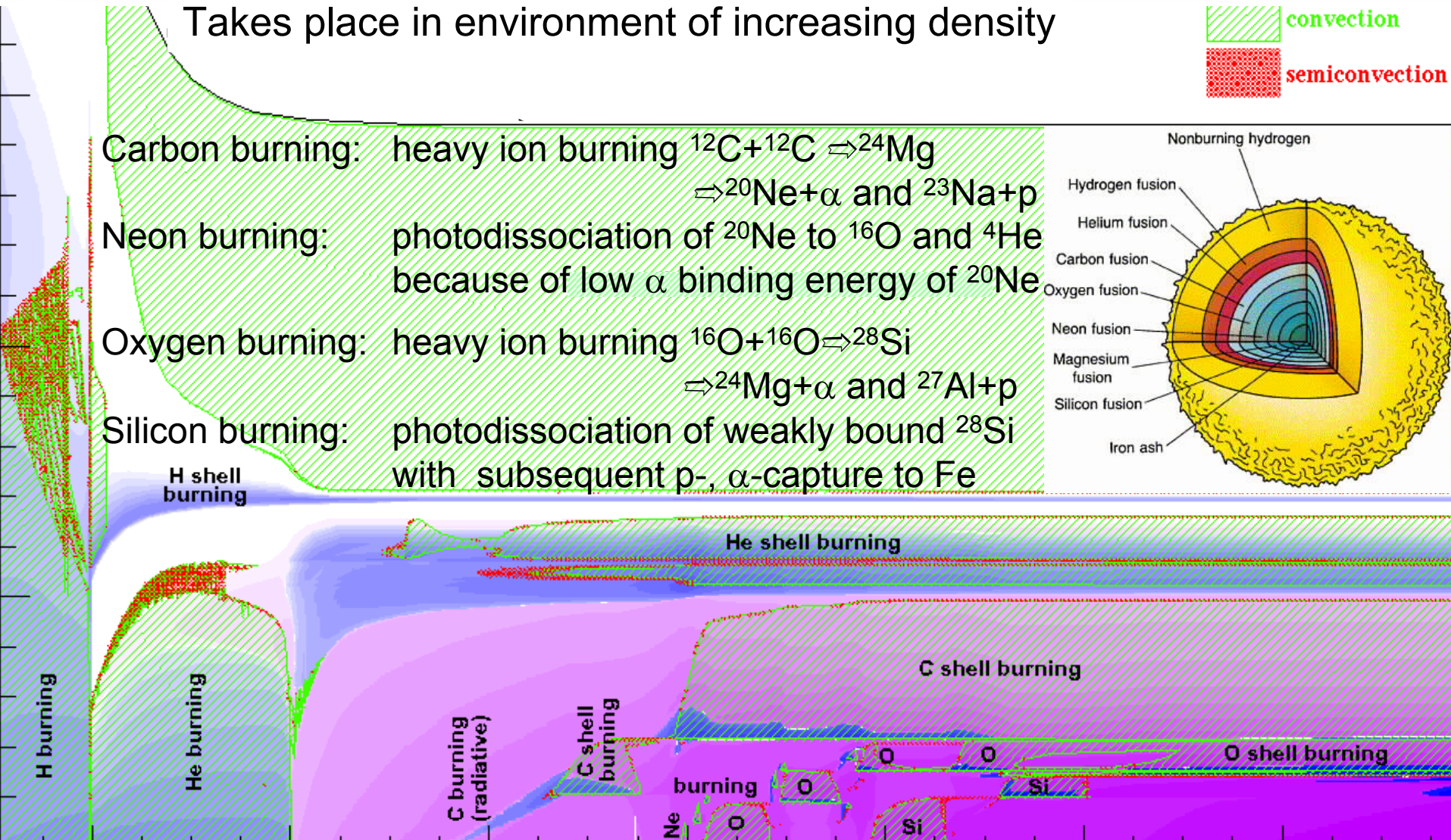
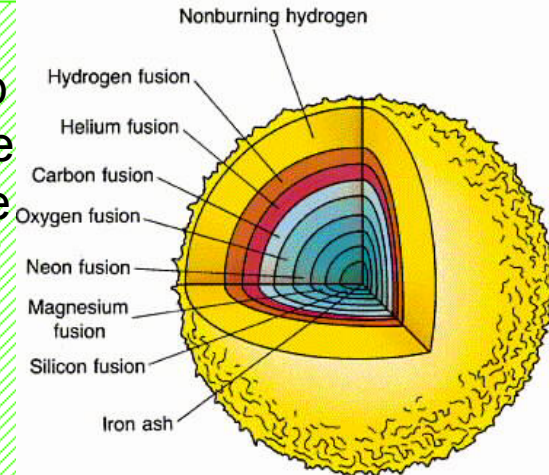
- ❑ post helium burning
- ❑ ignition of stellar carbon and oxygen burning
- ❑ nucleosynthesis in shell carbon burning
- ❑ from neon to silicon burning

Post-helium burning sequences

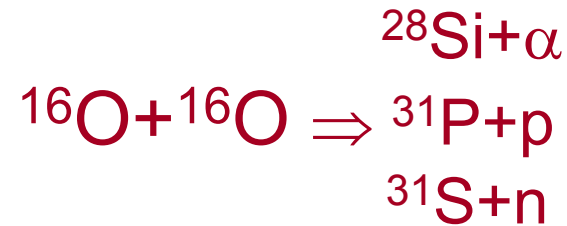
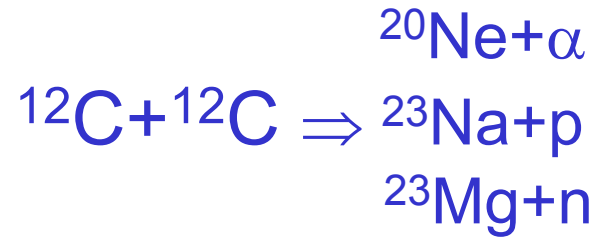
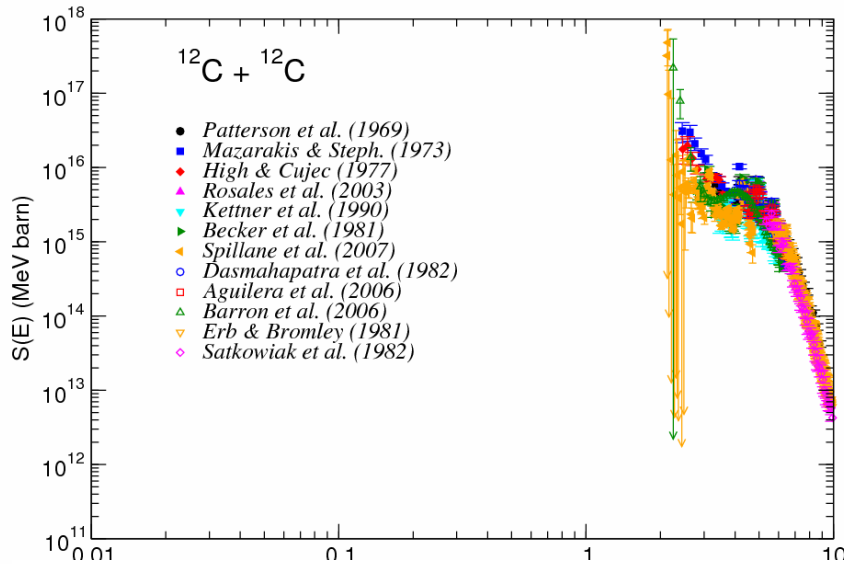
Takes place in environment of increasing density



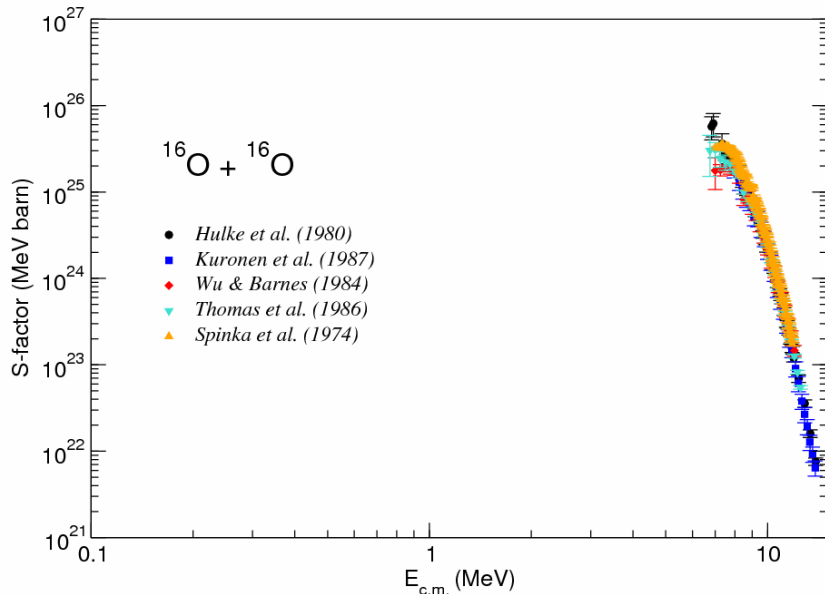
- Carbon burning: heavy ion burning $^{12}\text{C}+^{12}\text{C} \Rightarrow ^{24}\text{Mg}$
 $\Rightarrow ^{20}\text{Ne}+\alpha$ and $^{23}\text{Na}+\text{p}$
- Neon burning: photodissociation of ^{20}Ne to ^{16}O and ^4He
 because of low α binding energy of ^{20}Ne
- Oxygen burning: heavy ion burning $^{16}\text{O}+^{16}\text{O} \Rightarrow ^{28}\text{Si}$
 $\Rightarrow ^{24}\text{Mg}+\alpha$ and $^{27}\text{Al}+\text{p}$
- Silicon burning: photodissociation of weakly bound ^{28}Si
 with subsequent p-, α -capture to Fe



Problems of heavy ion burning



How to extrapolate, what are branchings



- Times scale for stellar C, O burning
- Neutron production in C-burning & weak s-process nucleosynthesis
- White dwarf abundance distribution & nucleosynthesis in Ne-novae
- Ignition conditions for type I SN
- Ignition condition for Superbursts

What potential model is appropriate?

Different potential models leads to different extrapolation of low energy cross section (S-factor).

Extreme case,

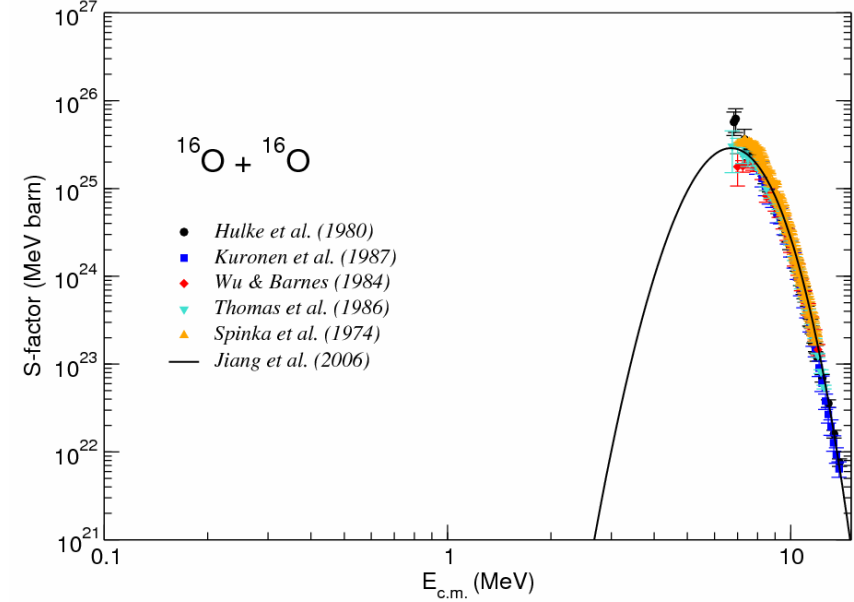
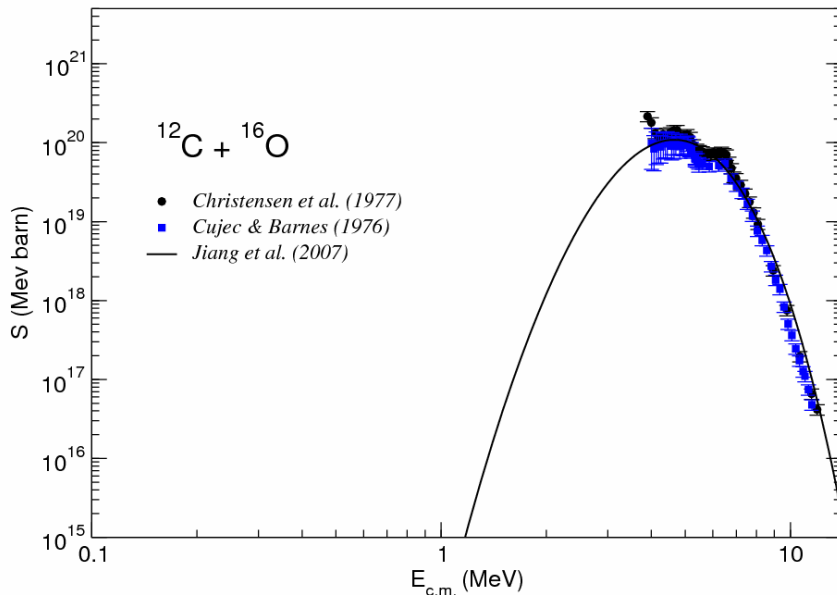
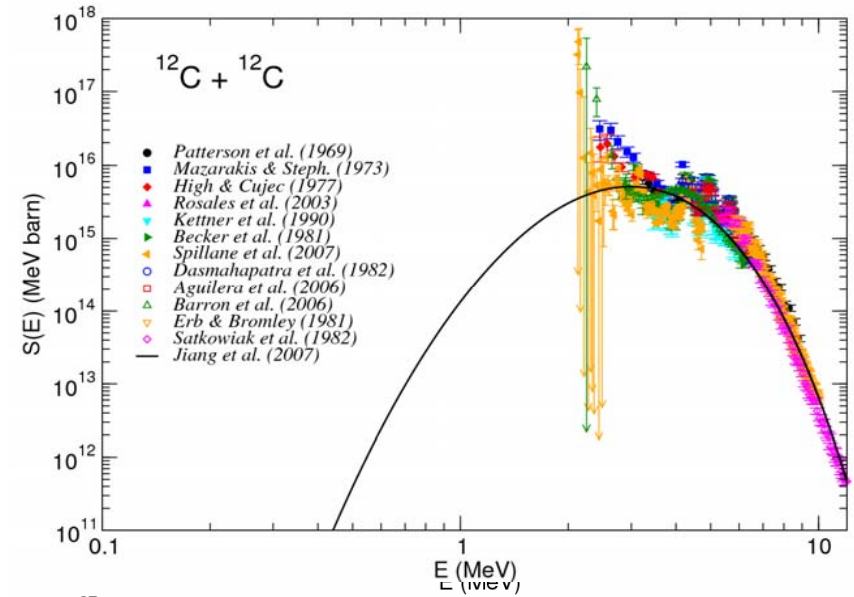
- standard potential model
- hindrance potential model

Caughlan & Fowler 1988

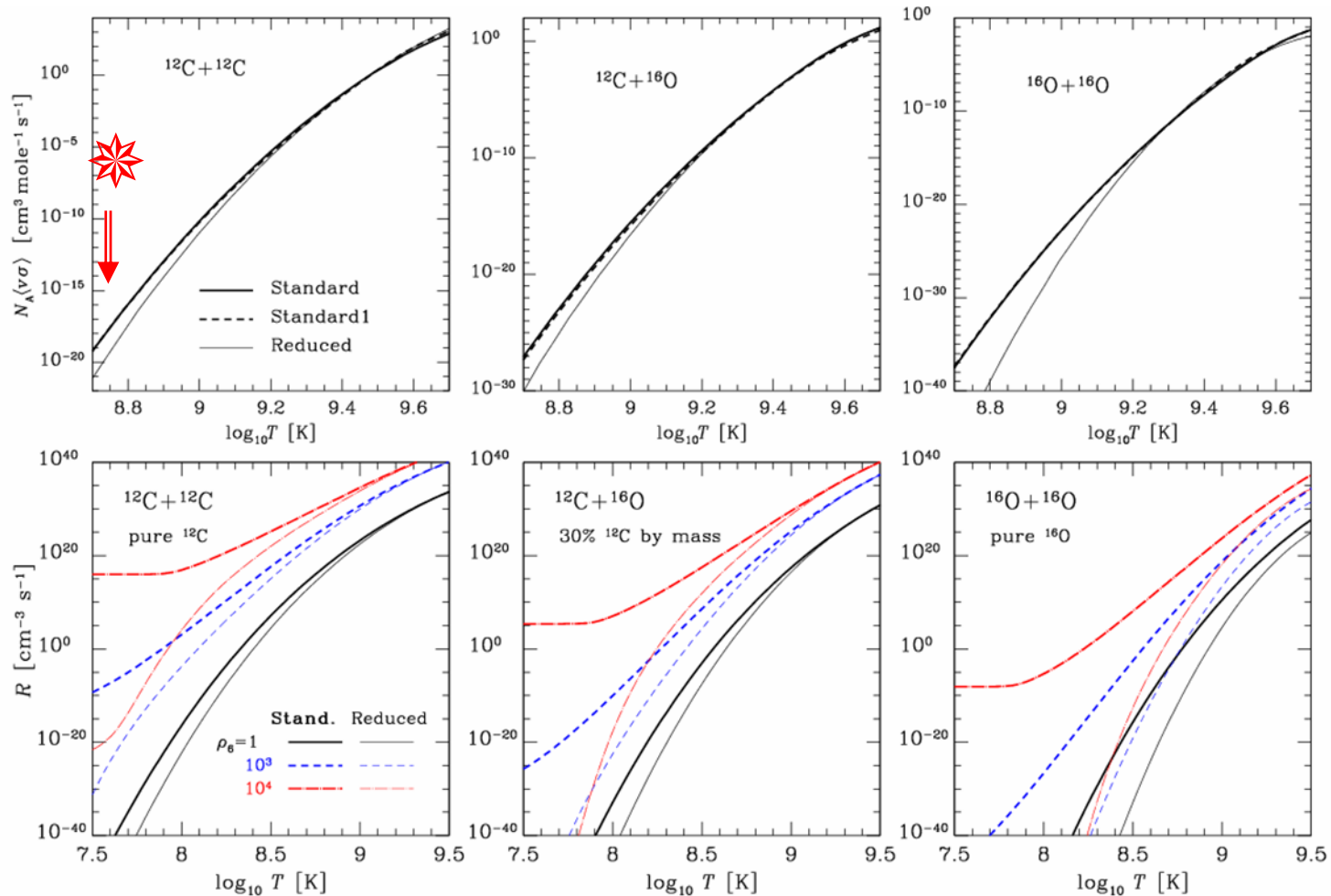
Gasques et al. 2005

Yakovlev et al. 2006

Jiang et al. 2007

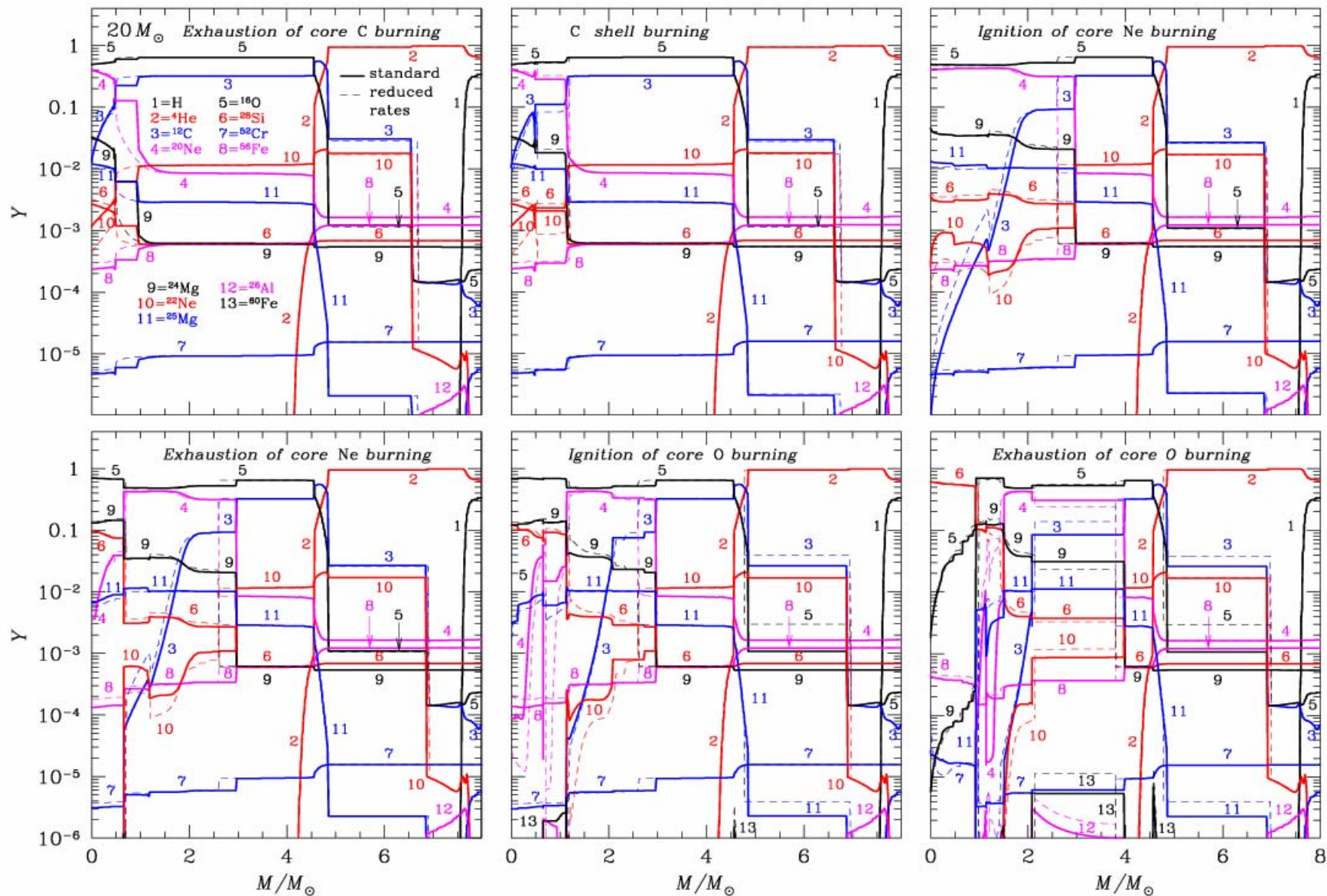


Density & Screening Dependence of Fusion

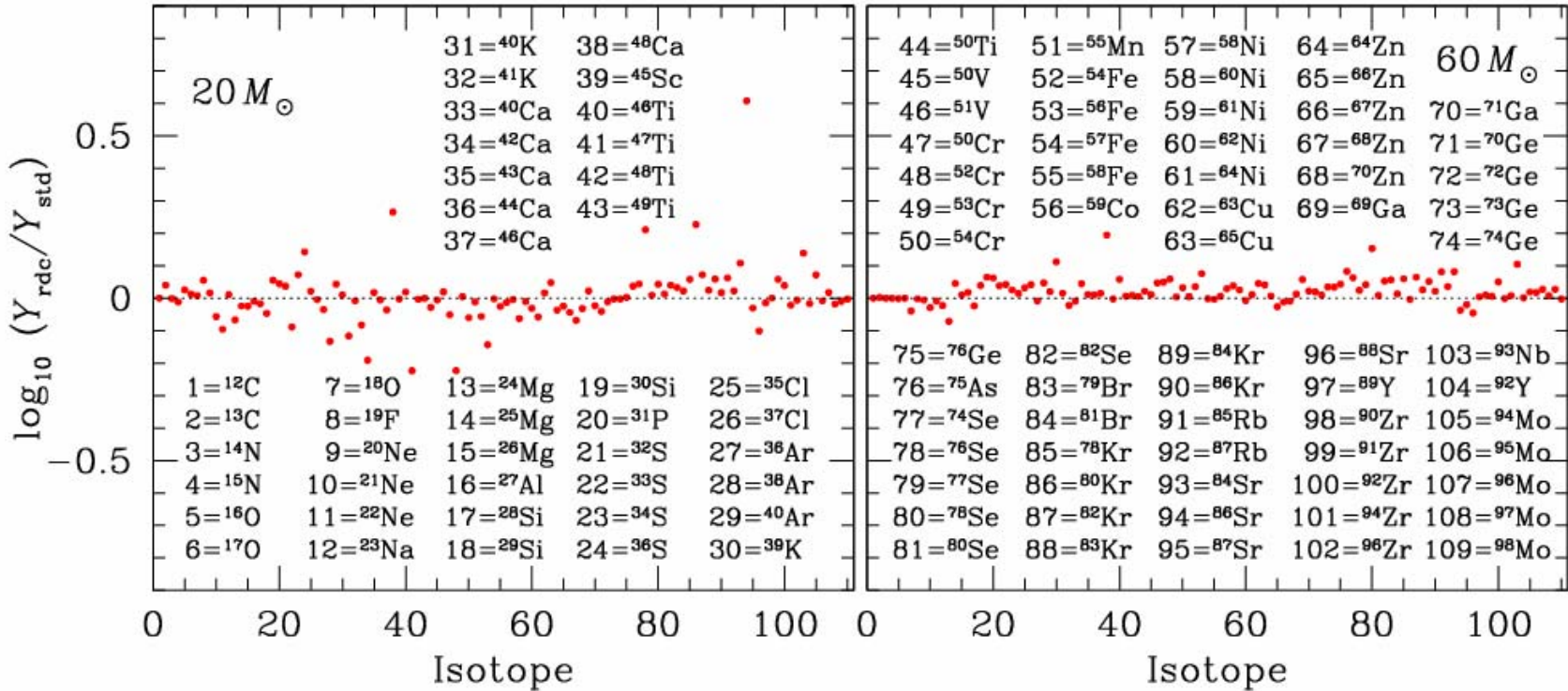


Towards higher densities there is an increase in the rate due to electron screening effects. The free electrons reduce the deflective Coulomb potential between the two fusing ions.

Abundance evolution in late stellar burning

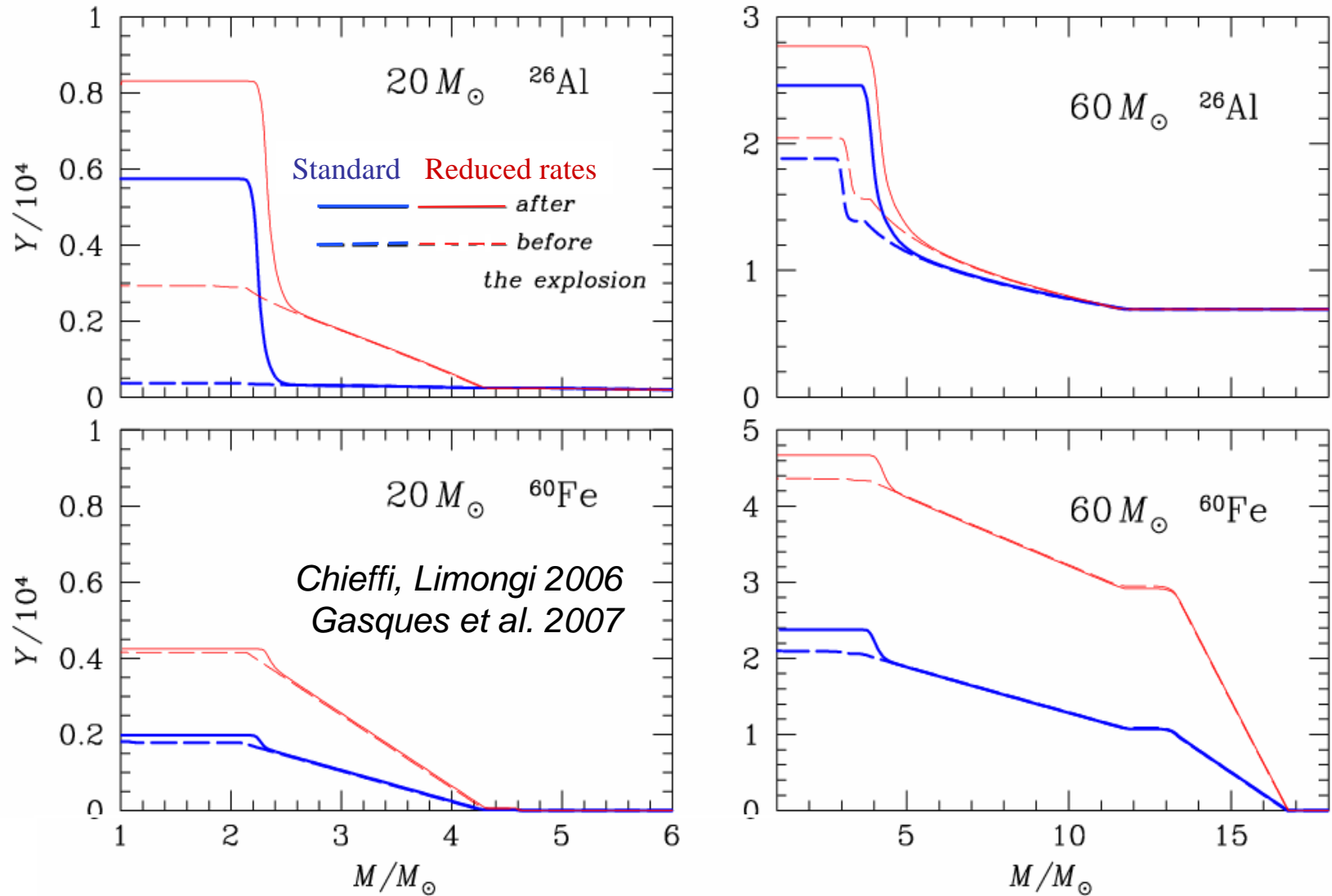


Consequences for late stellar burning

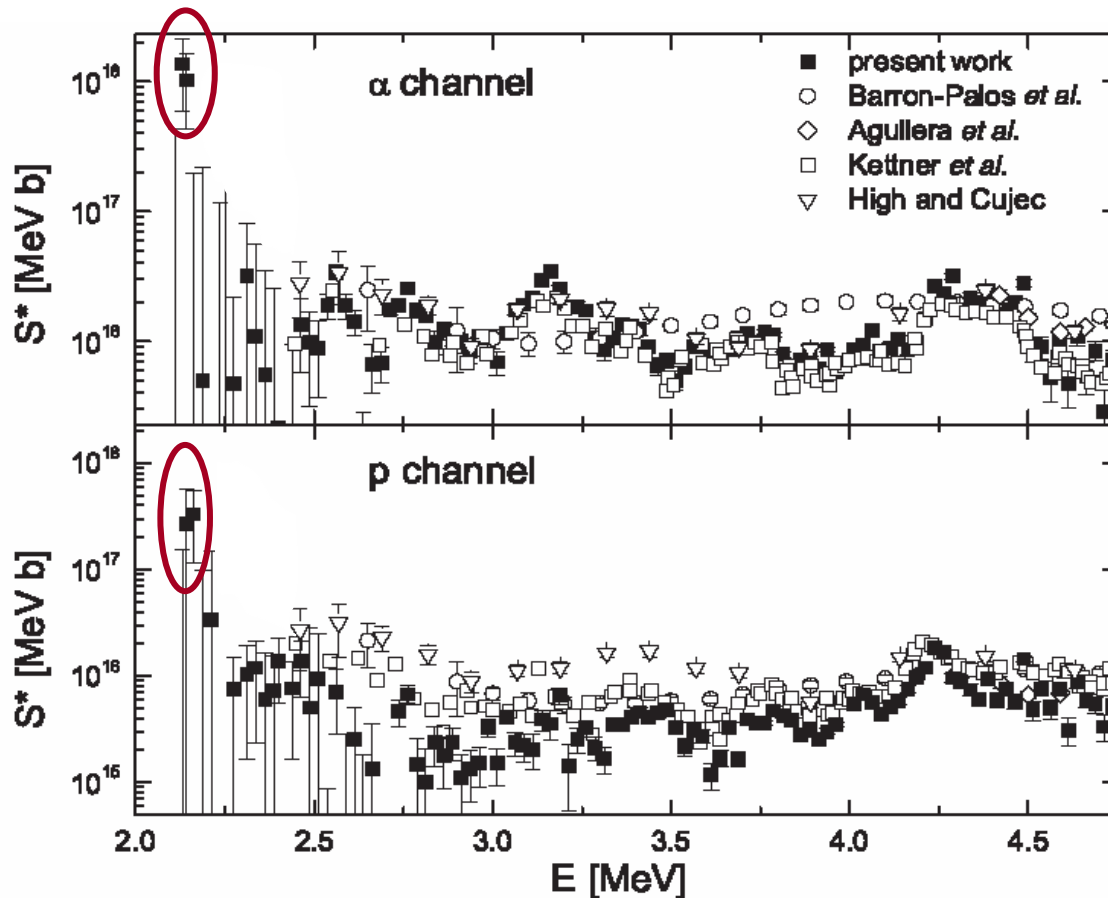


Simulations performed for 20 and $60 M_{\odot}$ stars, no major differences for nucleosynthesis except a significant increase in abundance for the long-lived radioactive isotopes ²⁶Al and ⁶⁰Fe and some s-process nuclei. This suggests impact on n production. That needs further investigation.

Production of Galactic Radioactivity?



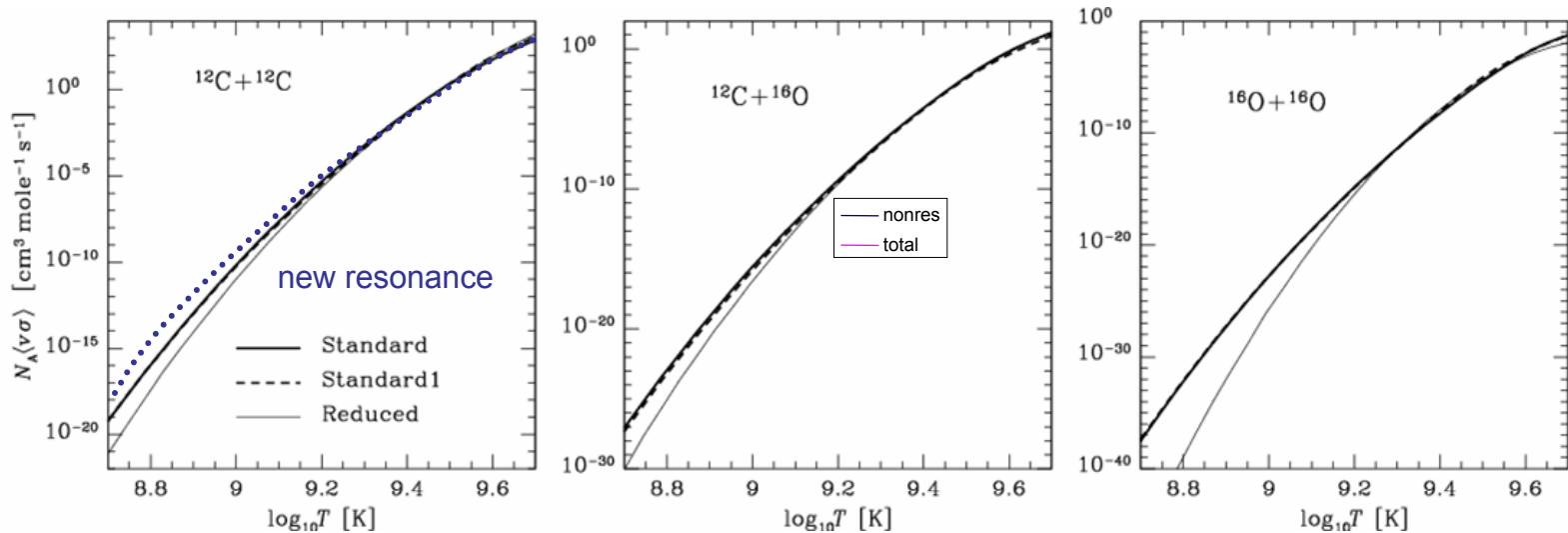
Resonance Structures in $^{12}\text{C}+^{12}\text{C}$



Recent data suggest strong but narrow resonance structures in the $^{12}\text{C}+^{12}\text{C}$ reaction system. The data point towards a ^{12}C configuration without a specific preference for the subsequent proton or alpha decay! The branching ratio is very uncertain.

Reaction rate formalism

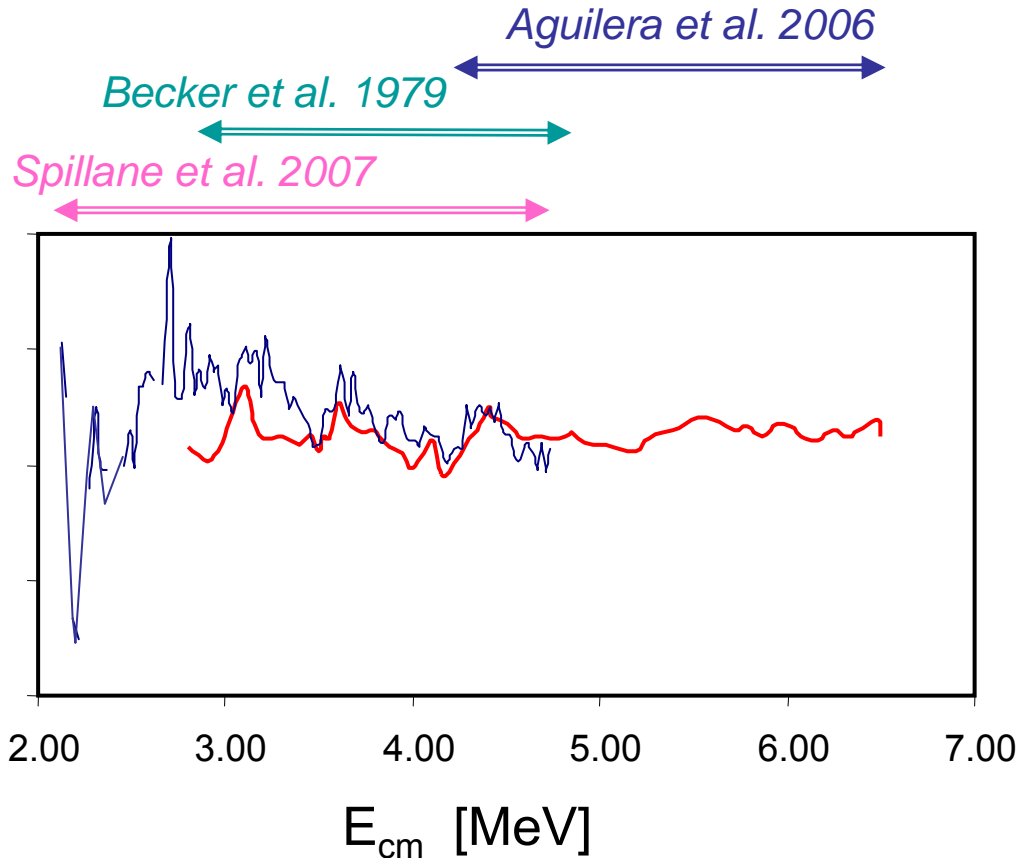
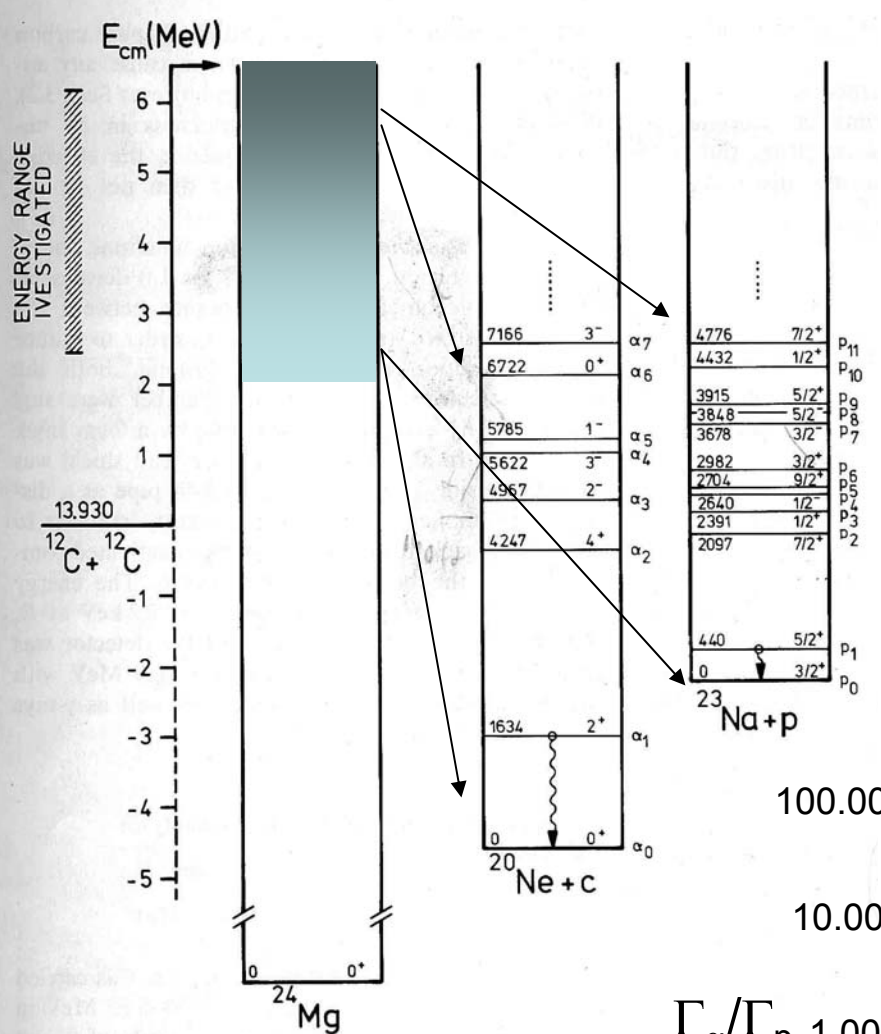
$$N_A \langle \sigma v \rangle = N_A \cdot f_{screen} \cdot \sqrt{\frac{2}{\mu}} \cdot \frac{\Delta E_G}{(kT)^{3/2}} \cdot S_{ij} \cdot e^{\left(-\frac{3E_G}{kT} \right)}$$



Additional resonance causes significant enhancement of low temperature rate, more resonances could contribute more strongly.

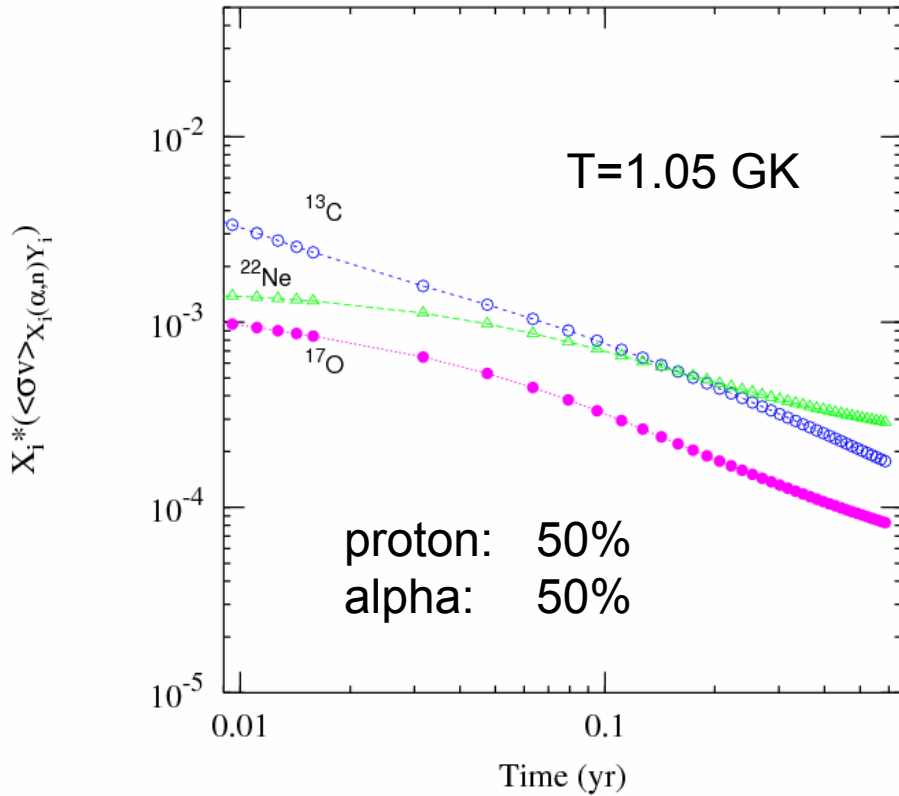
PROTON-ALPHA BRANCHING

Pronounced alpha and single particle level structure at lower energies expected!



On average $\Gamma_\alpha/\Gamma_p \approx 1.8!$
 But indication for α -cluster structure in ^{24}Mg is visible in resonance structure!

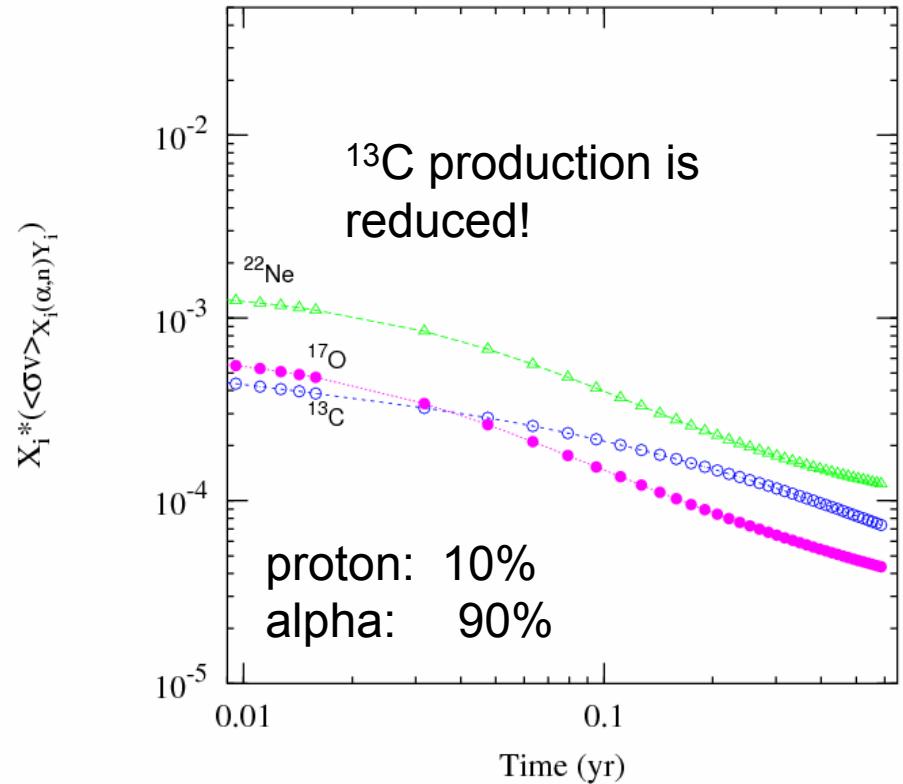
Consequences for Neutron Sources



$^{13}\text{C}(\alpha,n)$

^{13}C originates through $^{12}\text{C}(p,\gamma)^{13}\text{N}(\beta^+)^{13}\text{C}$

Pignatari et al. 2008 in preparation



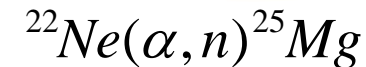
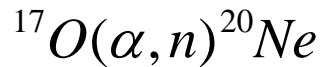
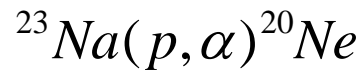
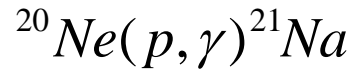
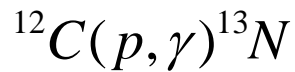
$^{17}\text{O}(\alpha,n)$ & $^{22}\text{Ne}(\alpha,n)$

^{22}Ne left from preceding He-burning

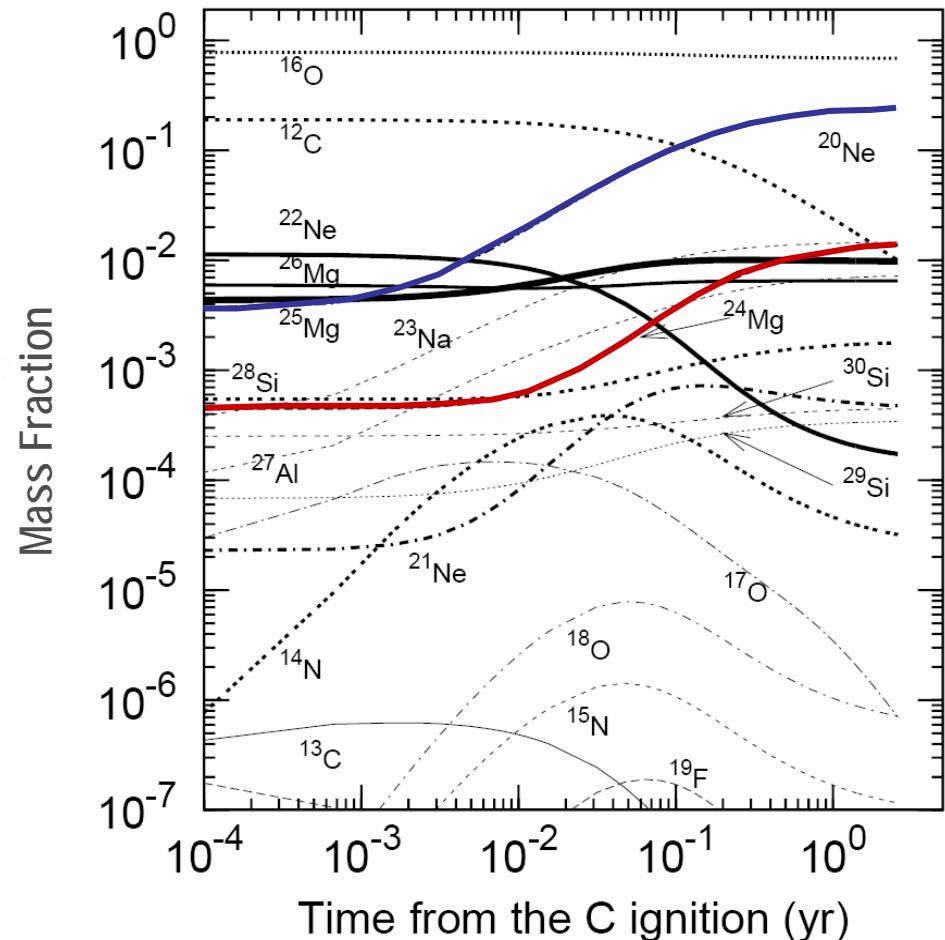
^{17}O originates through $^{16}\text{O}(n,\gamma)$

Subsequent light ion reactions in carbon burning environment

Release of protons and alphas during carbon burning:



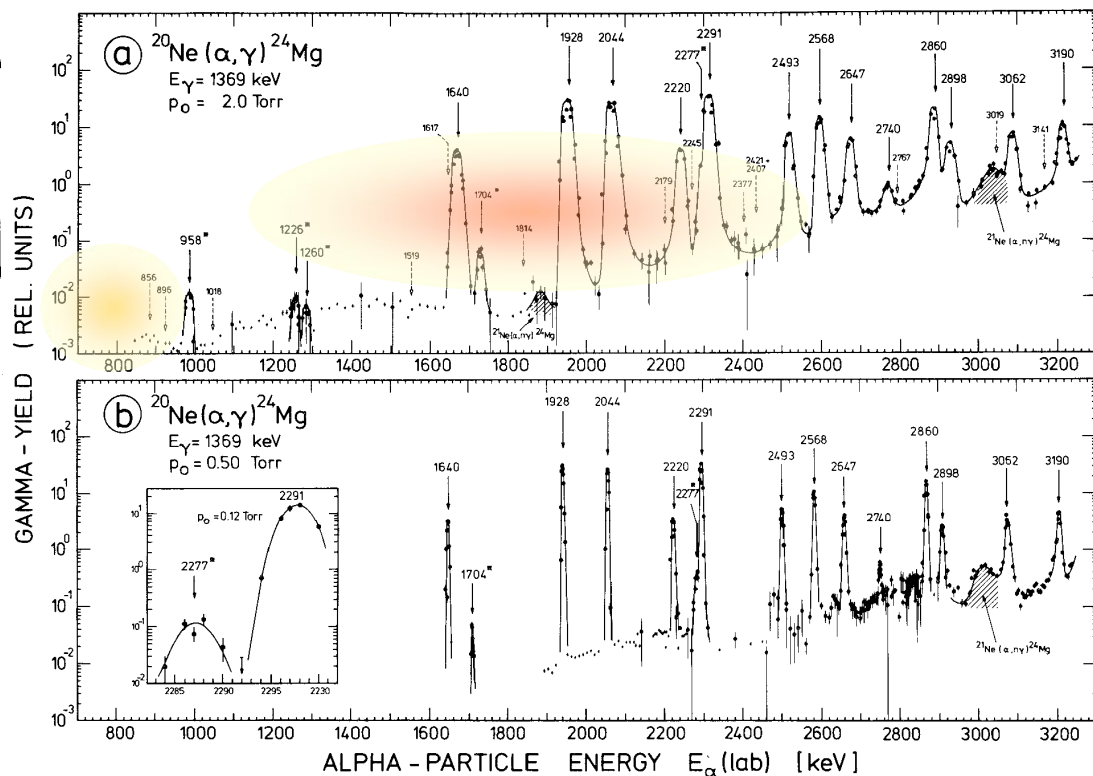
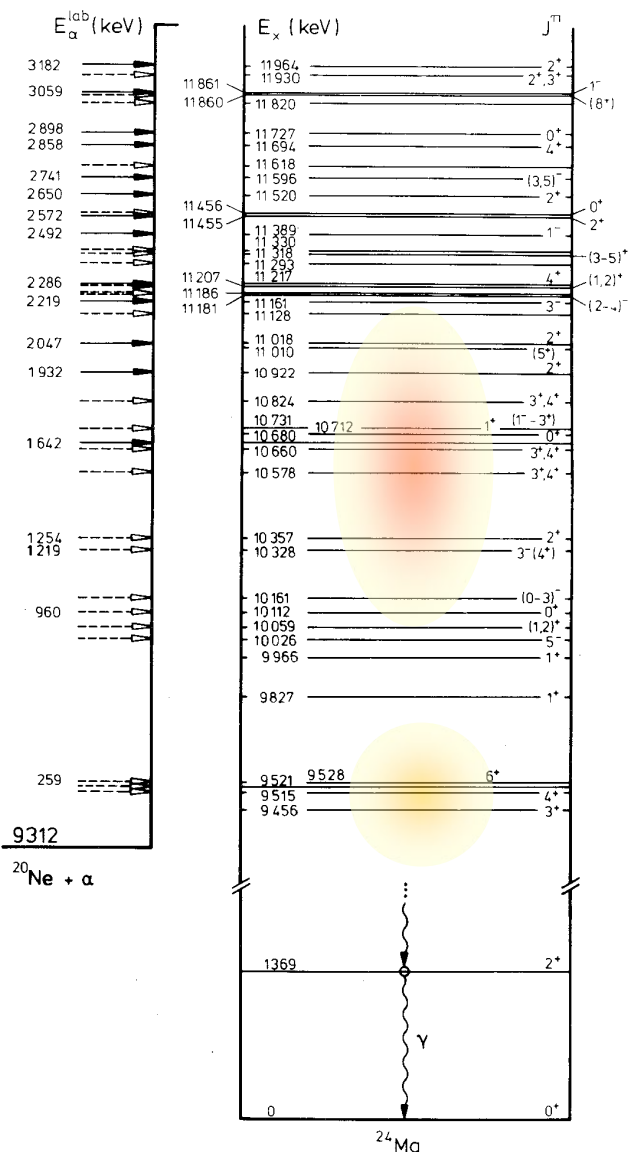
Alpha capture reactions are considerably weaker than proton capture! Subsequent nucleosynthesis depends critically on proton alpha emission associated with single particle/alpha cluster configuration of ^{24}Mg above the $^{12}\text{C}+^{12}\text{C}$ threshold.



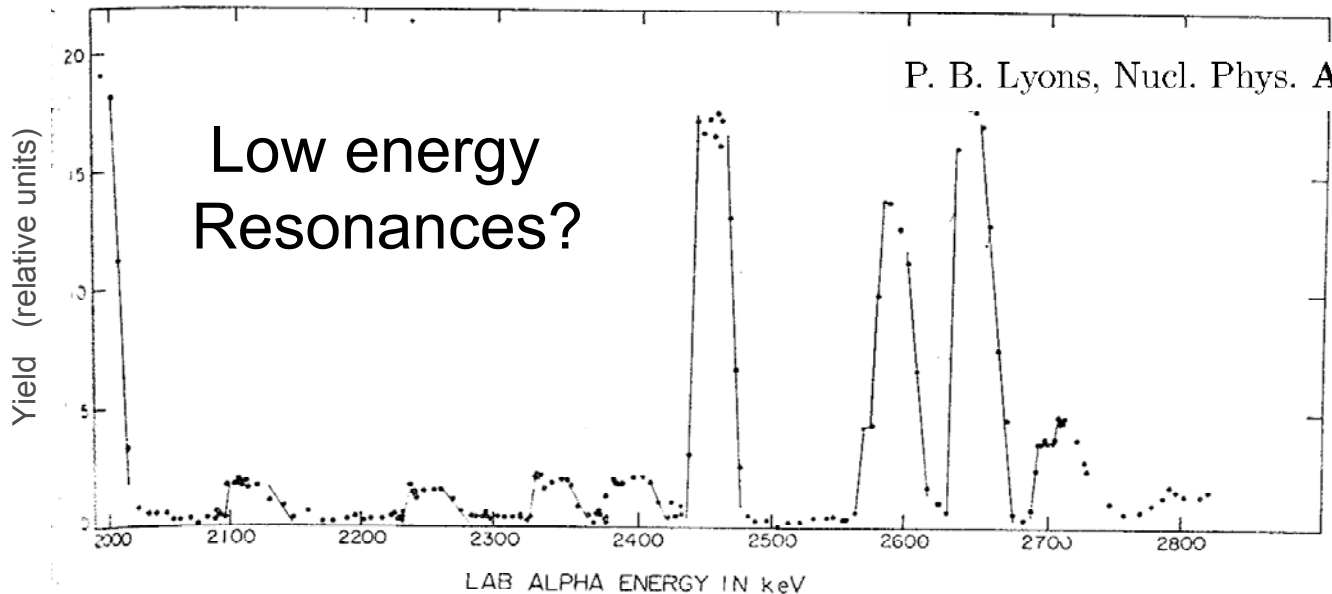
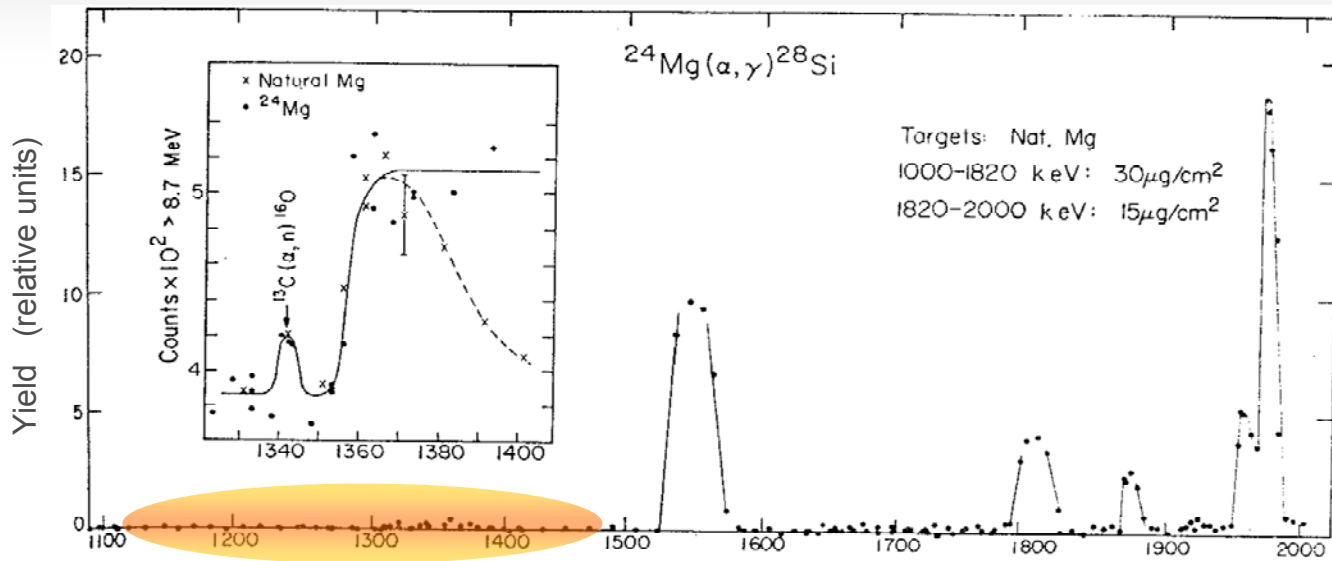
The $^{20}\text{Ne}(\alpha, \gamma)^{24}\text{Mg}$ reaction

$$E_G = 0.122 \cdot (Z_1^2 \cdot Z_2^2 \cdot \mu \cdot T_9^2)^{1/3} \text{ [MeV]}$$

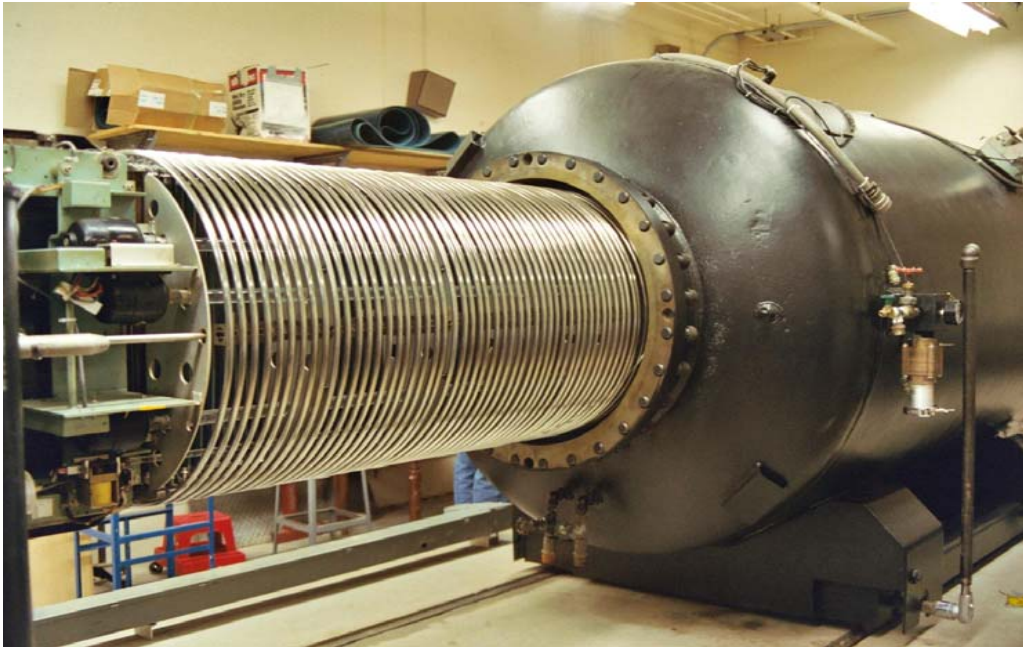
$$\Delta E_G = 0.236 \cdot (Z_1^2 \cdot Z_2^2 \cdot \mu \cdot T_9^5)^{1/6} \text{ [MeV]}$$



The $^{24}\text{Mg}(\alpha, \gamma)^{28}\text{Si}$ reaction



$^{24}\text{Mg}(\alpha, \gamma)^{28}\text{Si}$ at Notre Dame



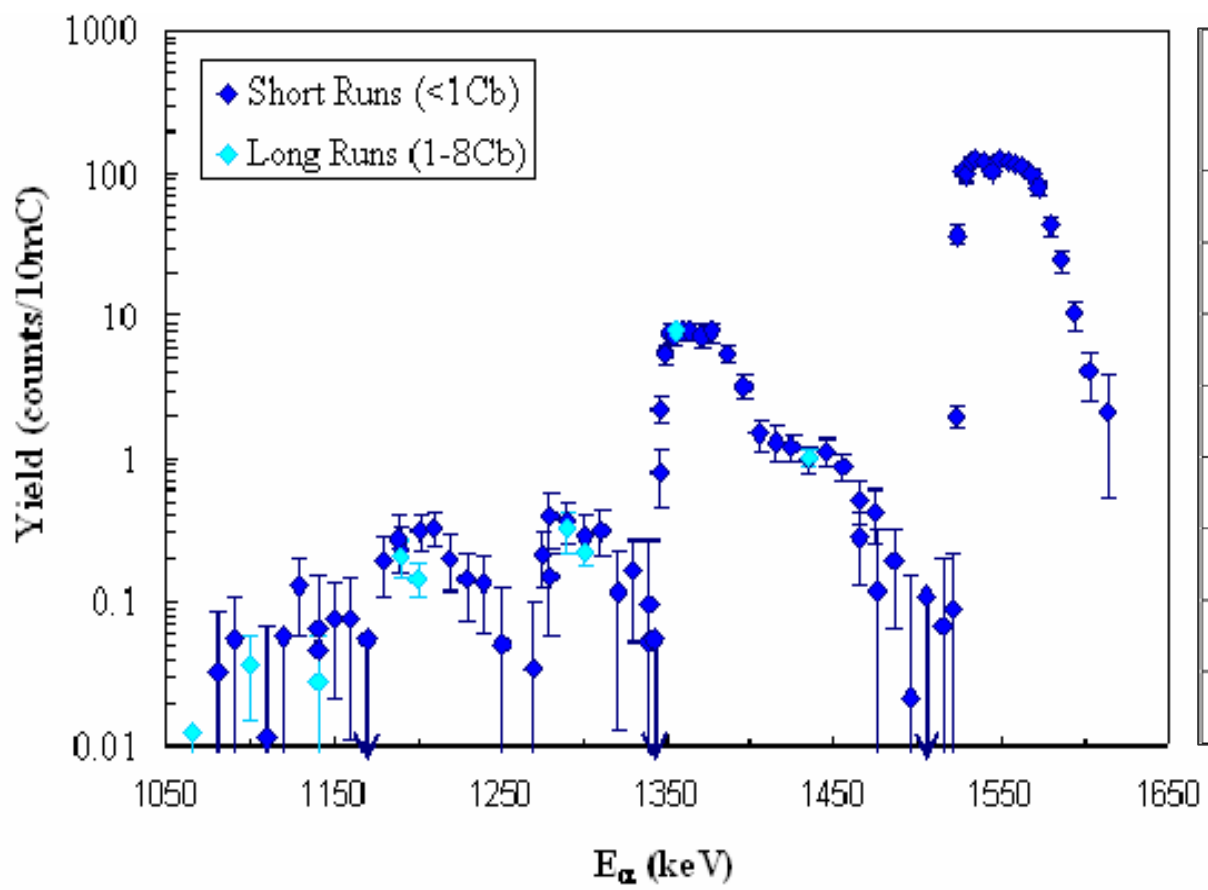
3.5 MV KN VdG accelerator
Beam of 50-150 μA on target

Natural Mg evaporated on Cu backing.
Long runs, with up to 20Cb charge
accumulation at low energies



NaI-Ge-Clover array. Active shielding
by coincidence requirement between
1.779 MeV ground state transition of
1st excited state in ^{28}Si (Ge) and the
primary resonance decays with
 $E_\gamma > 2.4$ MeV.

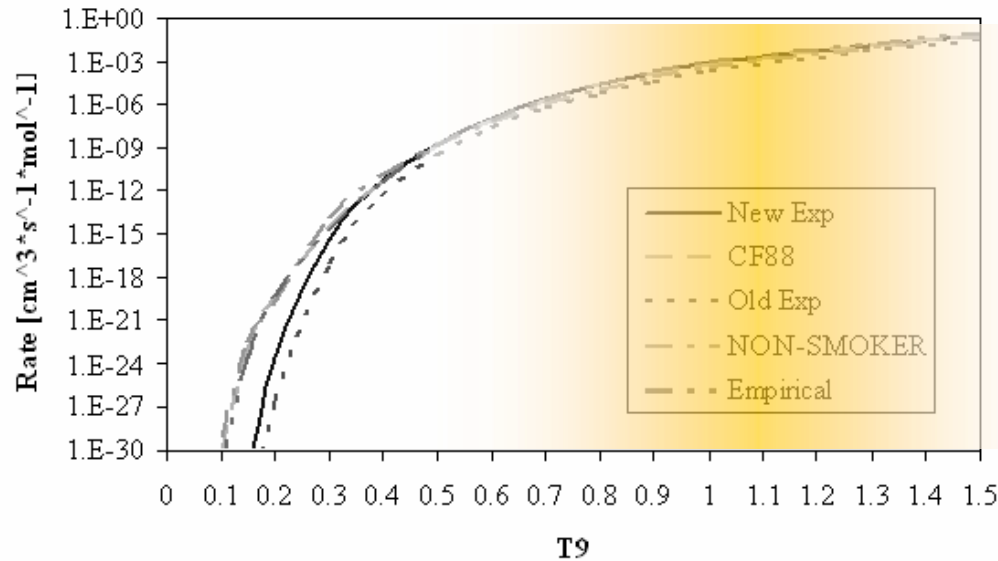
Thick Target Yield and Resonance Strength



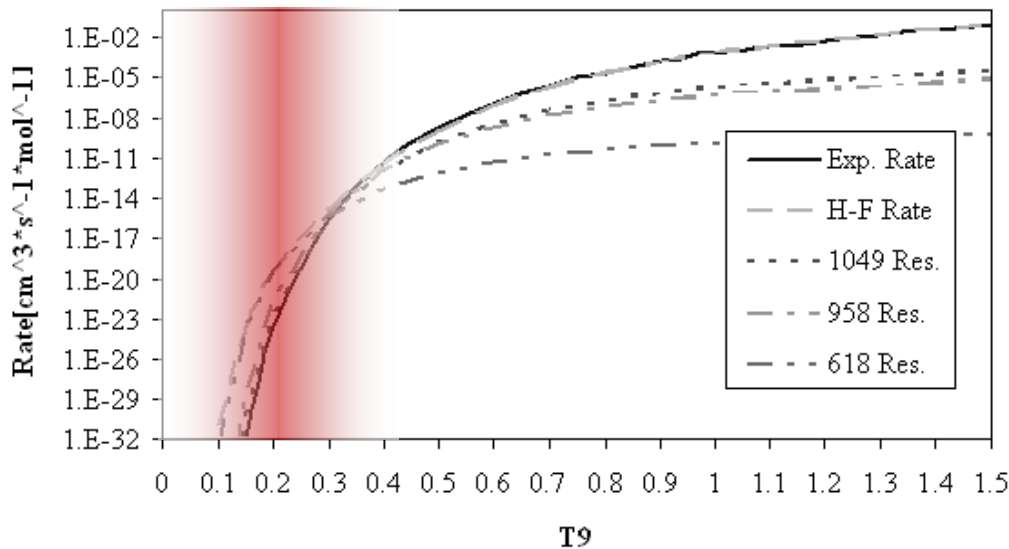
E_R (keV)	$\omega\gamma$ -this experiment (meV)	$\omega\gamma$ -previous value (meV)
1530	94 ± 14	110 ± 20
1413	0.21 ± 0.04	—
1351	1.9 ± 0.3	1.9 ± 0.6
1277	0.058 ± 0.011	—
1178	0.22 ± 0.06	—
1120/1130	<0.016	—
1087	<0.014	—
<1060	<0.002	—

New low energy resonances found, but considerable uncertainties remain!

Reaction Rate

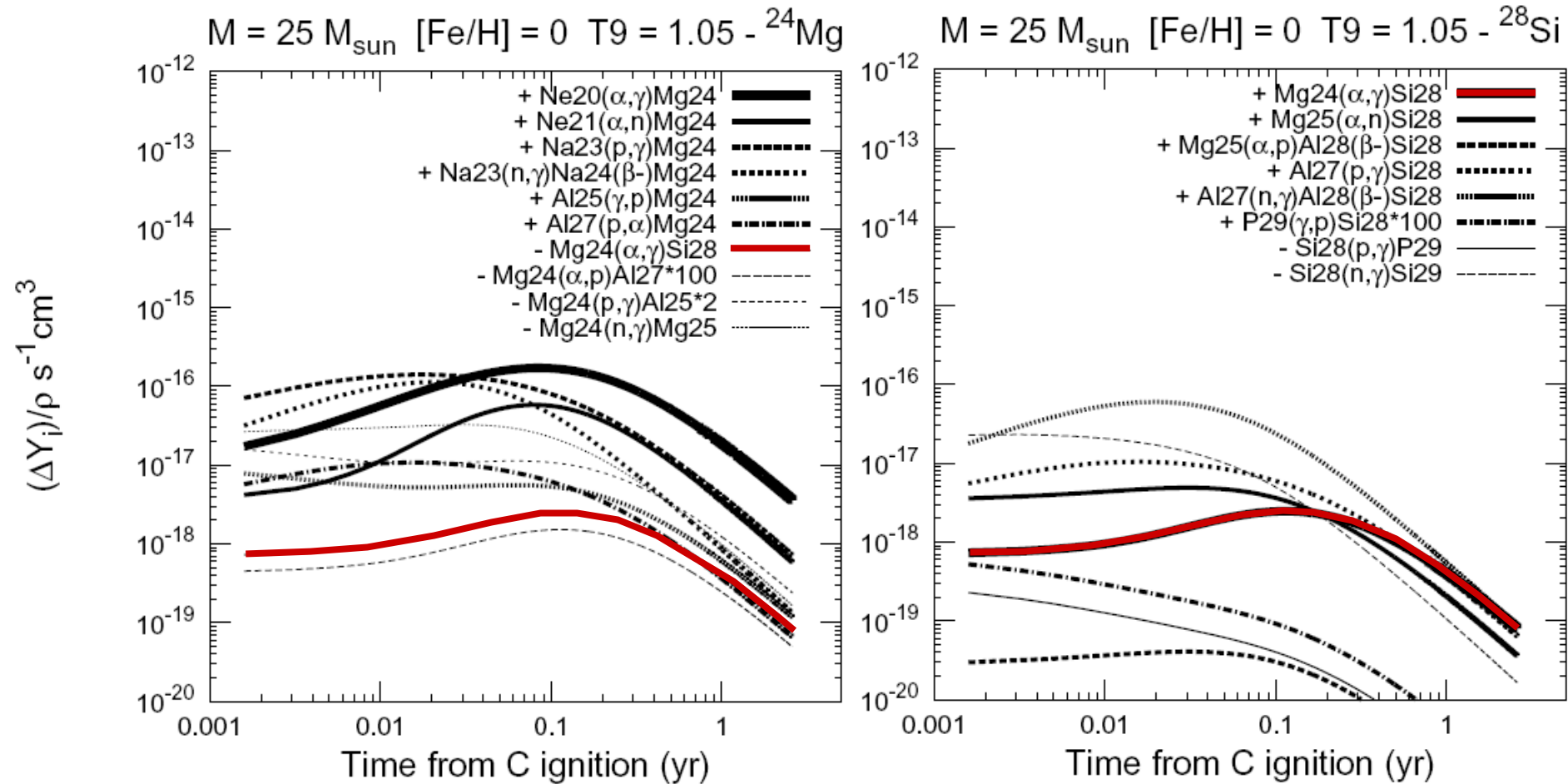


Experimental results indicate a slight enhancement of the rate in the temperature range of stellar carbon burning of $\sim 0.8\text{-}1.5\text{GK}$.



Estimated contributions of lower energy resonances (based on known natural parity states in ^{28}Si) indicate an enhancement of the rate in comparison to Hauser-Feshbach predictions at typical temperatures of stellar He burning.

Total flux for reactions forming or depleting ^{24}Mg , forming ^{28}Si in shell carbon burning



Strongest ^{24}Mg depletion reaction is $^{24}\text{Mg}(n, \gamma)^{25}\text{Mg}$

Strongest ^{28}Si production is $^{24}\text{Mg}(\alpha, \gamma)$ & $^{25}\text{Mg}(\alpha, n)^{28}\text{Si}$

On-site neutron production by (α, n) reactions

$^{22}\text{Ne}(\alpha, n)$

$^{17}\text{O}(\alpha, n)$

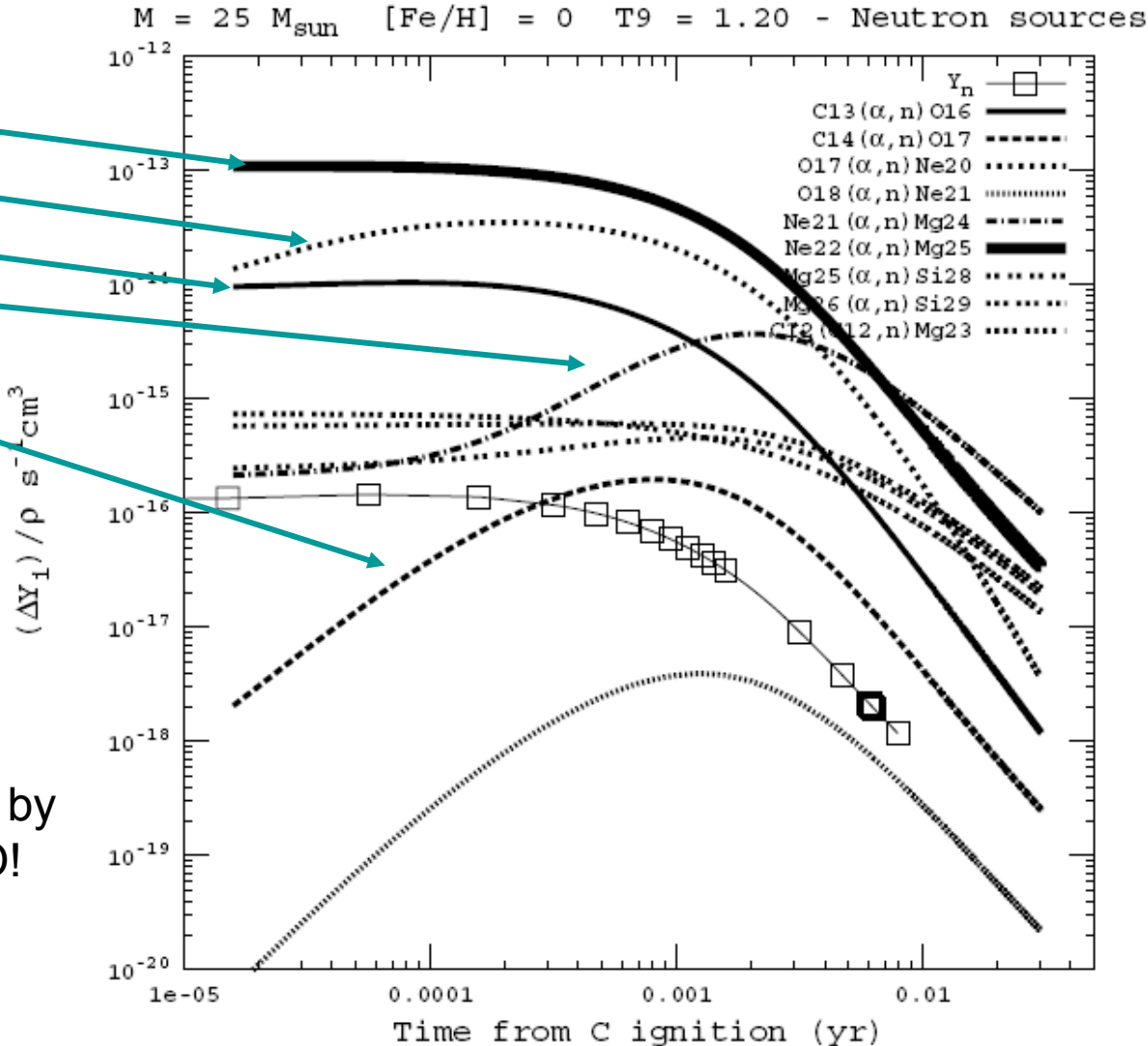
$^{13}\text{C}(\alpha, n)$

$^{21}\text{Ne}(\alpha, n)$

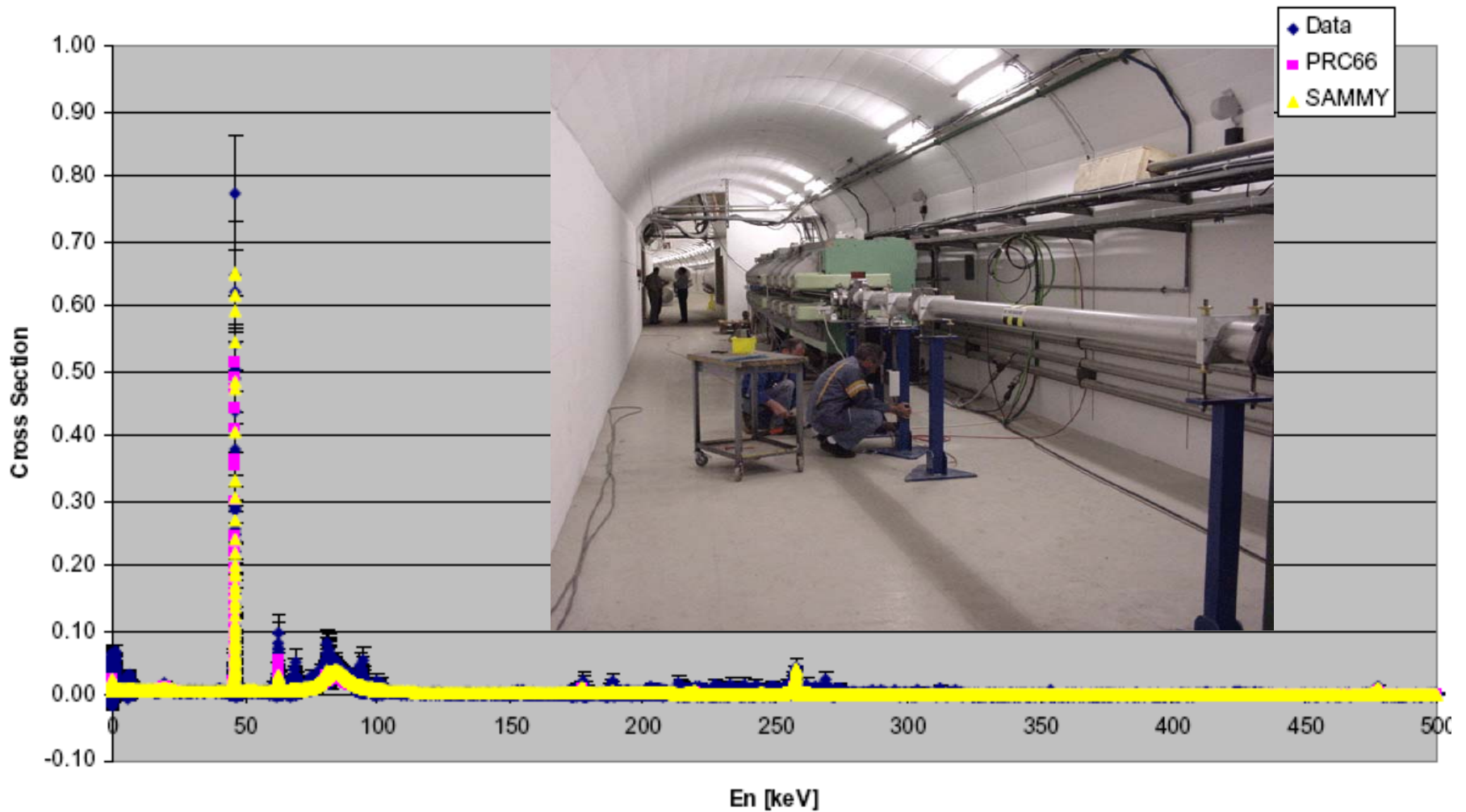
$^{14}\text{C}(\alpha, n)$

^{13}C , ^{17}O , ^{21}Ne , ^{22}Ne are the main neutron sources!

- ^{22}Ne is left over from preceding He burning!
- ^{13}C , ^{17}O are produced on site by proton capture on ^{12}C and ^{16}O !
- ^{21}Ne is produced by alpha capture sequence on ^{14}N

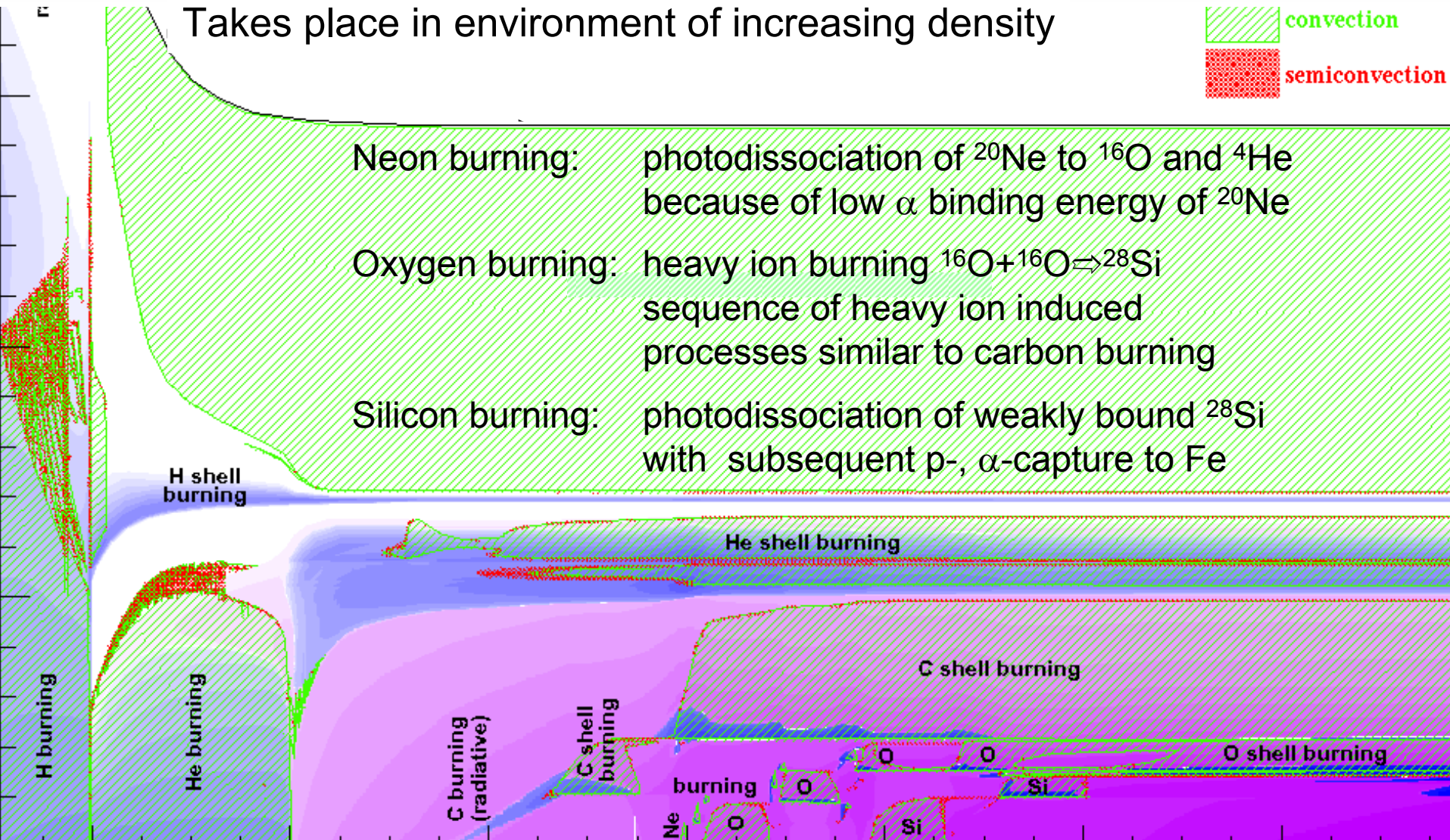


$^{24}\text{Mg}(n,\gamma)^{25}\text{Mg}$ branch



Recent n_ToF experiment yielded higher resonance strength.

Subsequent burning sequences



Neon burning

$^{20}\text{Ne}(\gamma, \alpha)^{16}\text{O}$	$Q = -4.73 \text{ MeV}$	Release of α particles through photodissociation of weakly bound ^{20}Ne ((α, γ) - (γ, α) -equilibrium?) and subsequent α capture induced nucleosynthesis along the T=0 line. (α -cluster structure effects)
$^{16}\text{O}(\alpha, \gamma)^{20}\text{Ne}$	$Q = 4.730 \text{ MeV}$	
$^{20}\text{Ne}(\alpha, \gamma)^{24}\text{Mg}$	$Q = 9.316 \text{ MeV}$	
$^{24}\text{Mg}(\alpha, \gamma)^{28}\text{Si}$	$Q = 9.984 \text{ MeV}$	

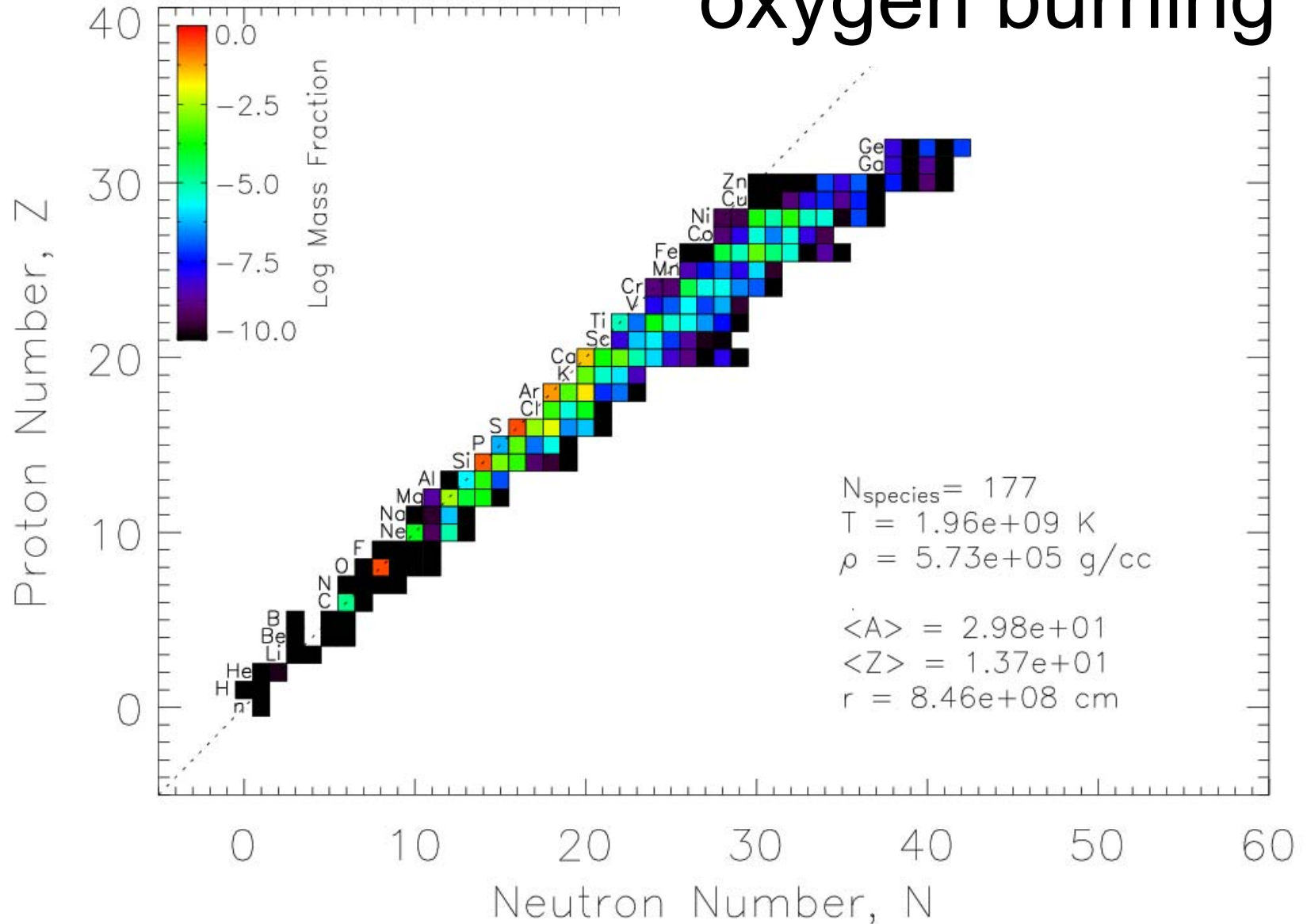
Oxygen burning

temperature at $T \approx 2$ GK; Gamow range at $E_G \approx 6 \pm 2$ MeV



Like in carbon burning, release on protons, alphas, and neutrons which change abundance conditions through subsequent capture processes at high energies \Rightarrow enrichment in ${}^{28}\text{Si}$ because of a presumably weak ${}^{28}\text{Si}(\alpha, \gamma){}^{32}\text{S}$ reaction rate.

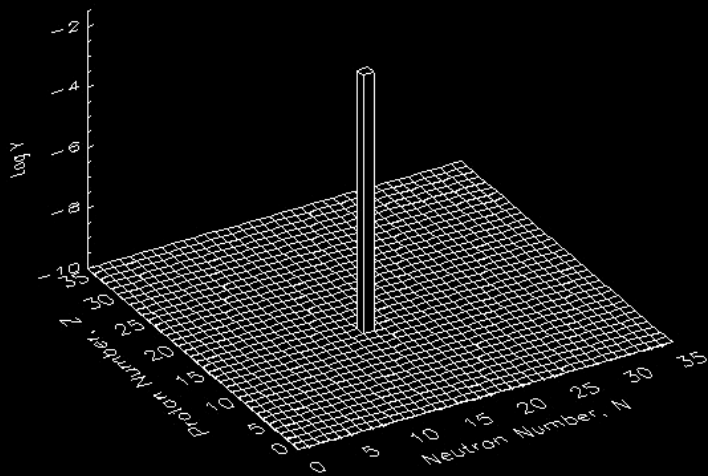
Abundance distribution after stellar oxygen burning



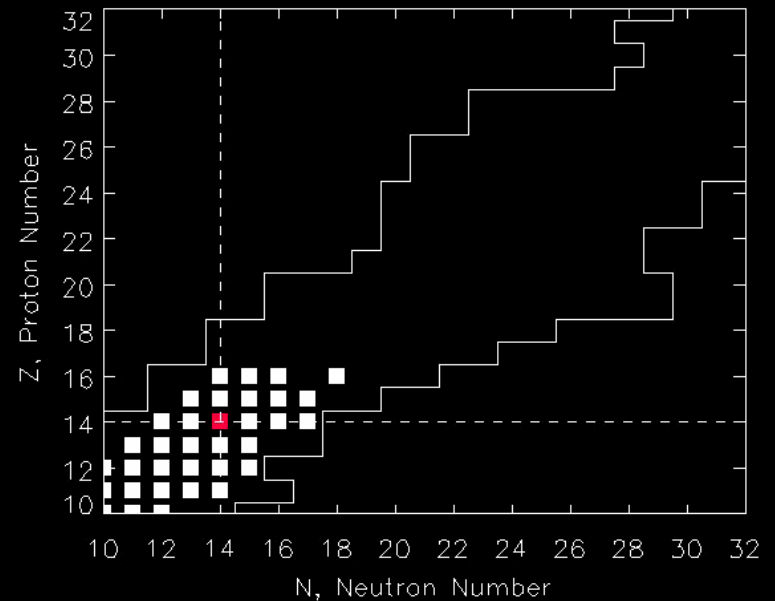
Si-burning

Photodissociation of ^{28}Si with subsequent build-up of heavy elements up to iron in statistical equilibrium
All reactions are balanced and the rates cancel out!

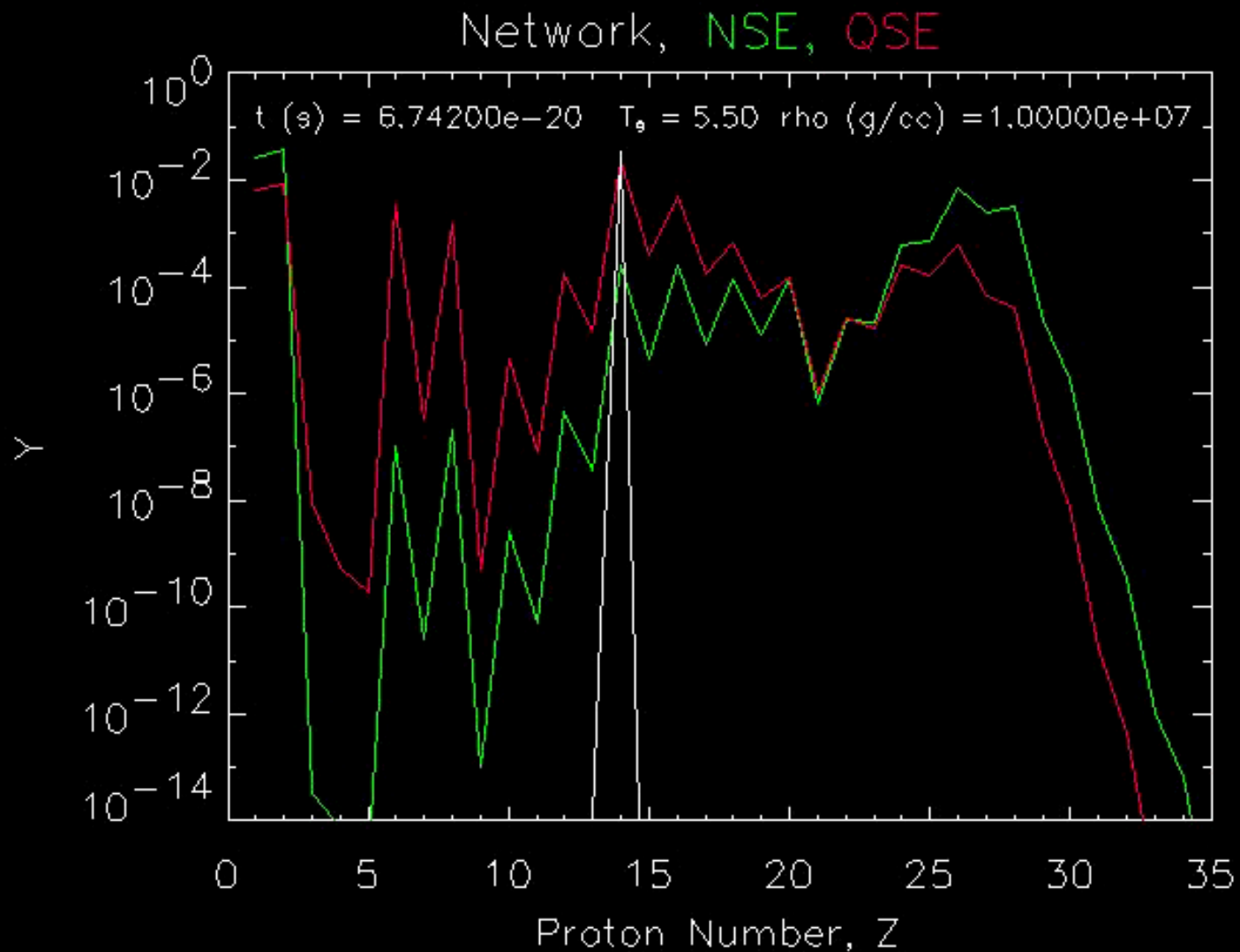
$t \text{ (s)} = 6.74200\text{e-}20$ $T_9 = 5.50$ $\rho \text{ (g/cc)} = 1.00000\text{e+}07$



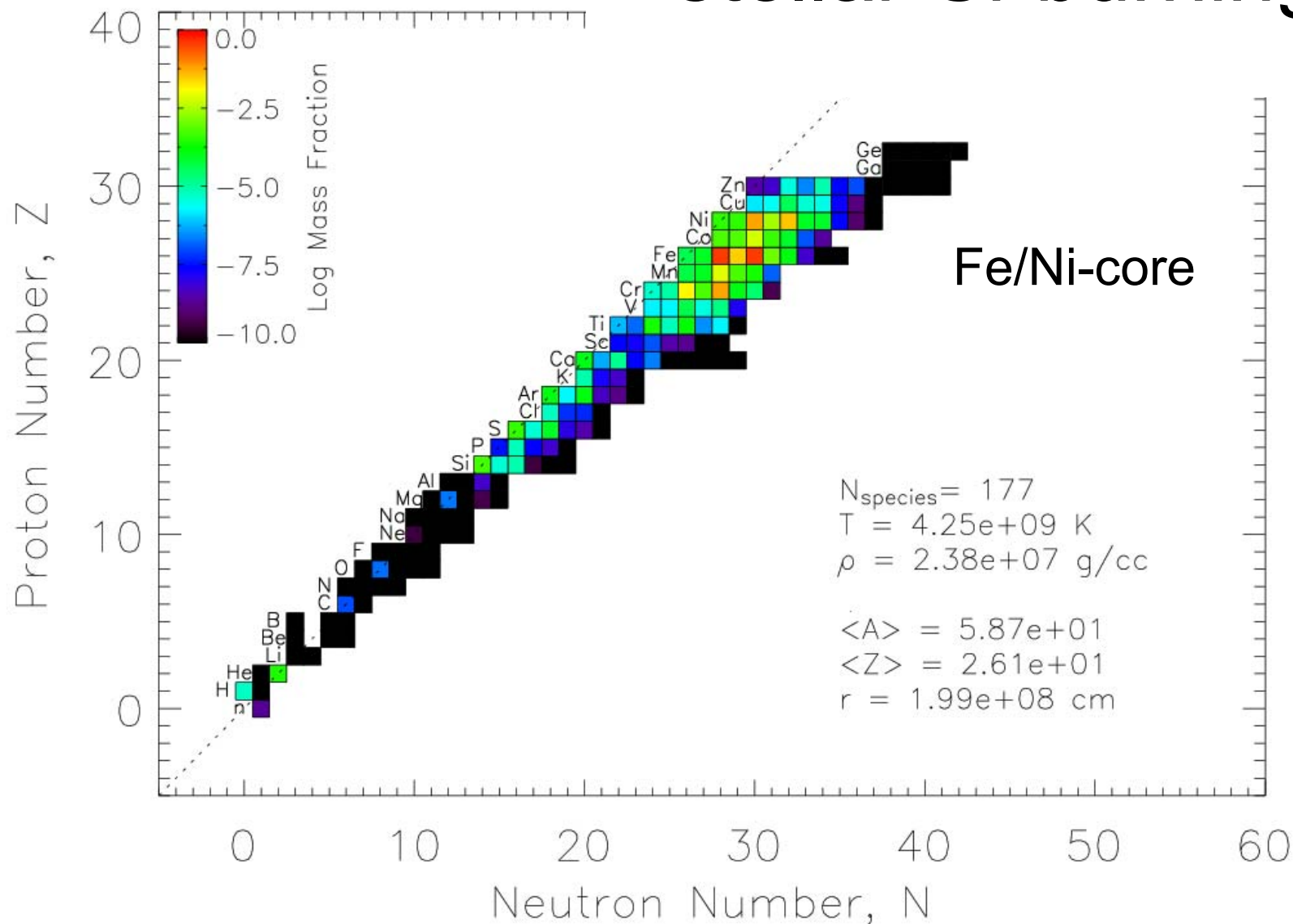
$t \text{ (s)} = 6.74200\text{e-}20$ $T_9 = 5.50$ $\rho \text{ (g/cc)} = 1.00000\text{e+}07$



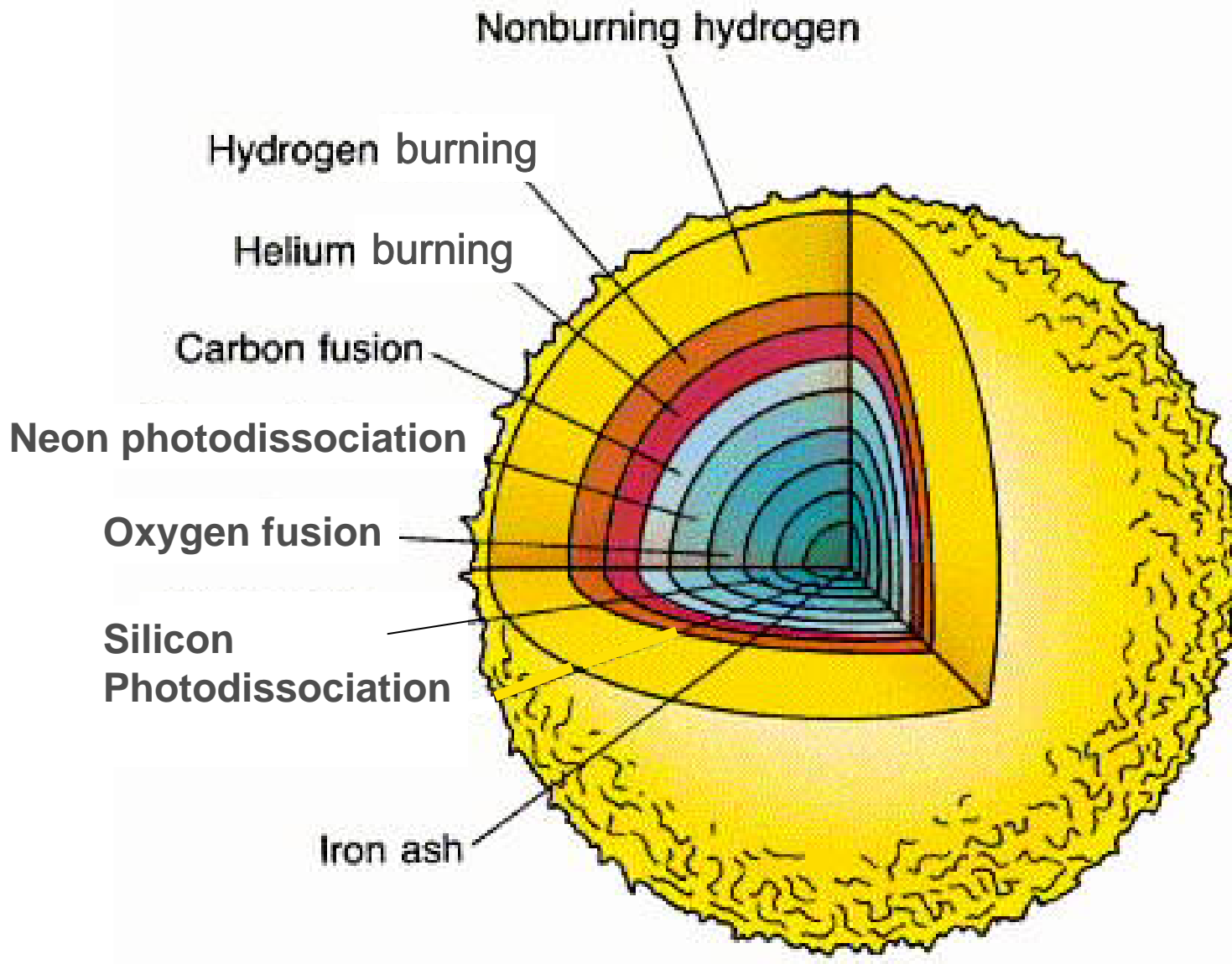
Si burning abundance evolution



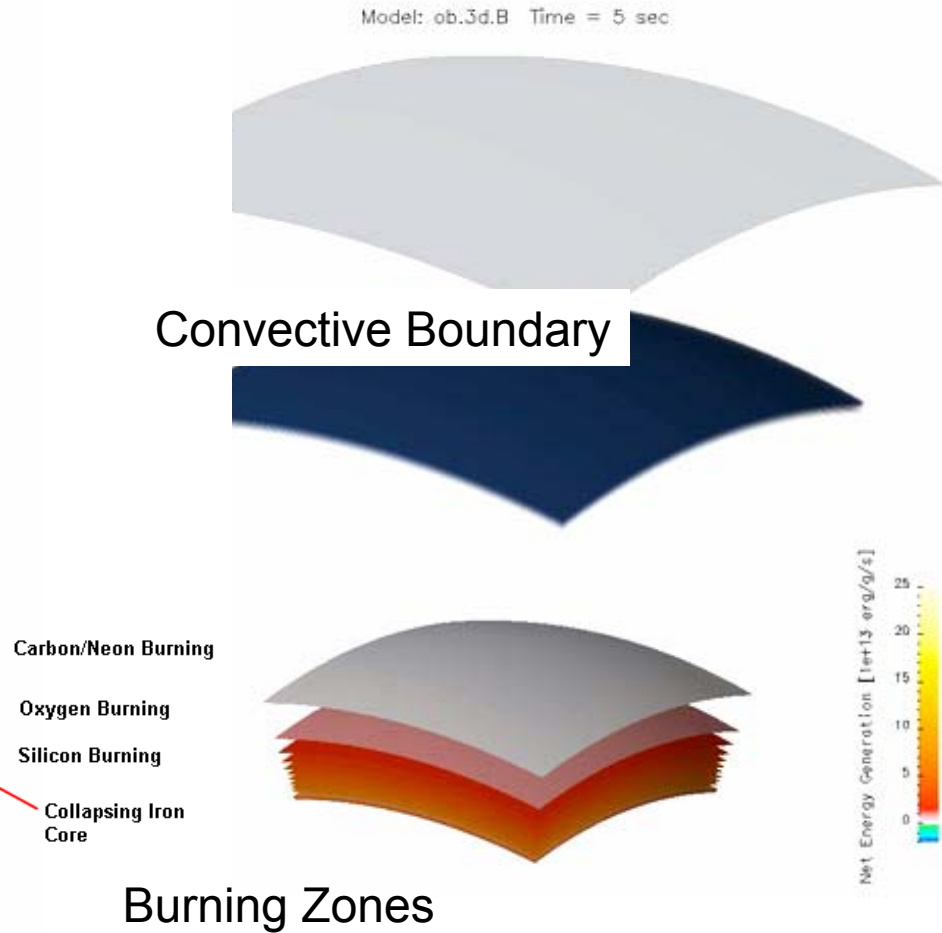
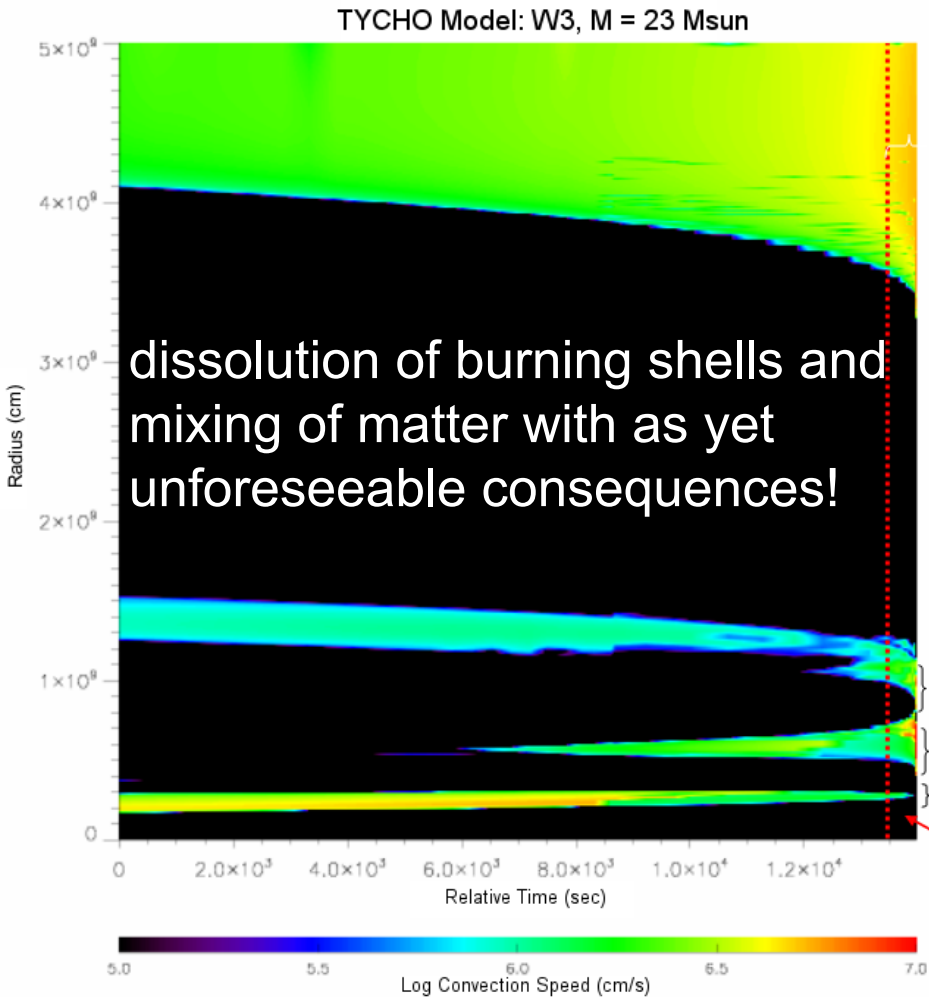
Abundance distribution in core after stellar Si-burning



The stellar Onion Model



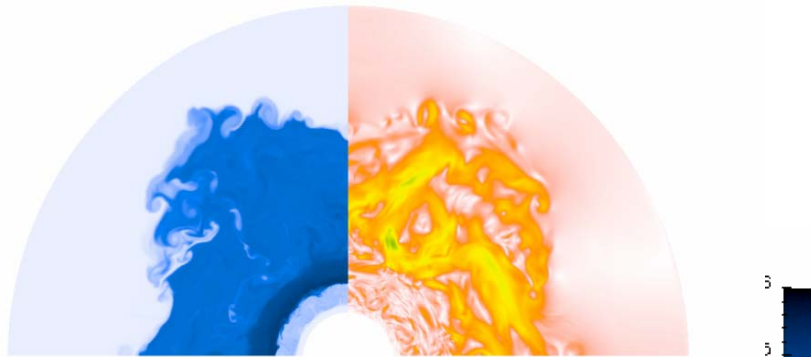
The last Days of Stellar Burning



Shell Burning and Shell Mixing

Casey Meakin & David Arnett (2006)

Shell burning takes place in moving blobs of material, rather than in well defined shells.



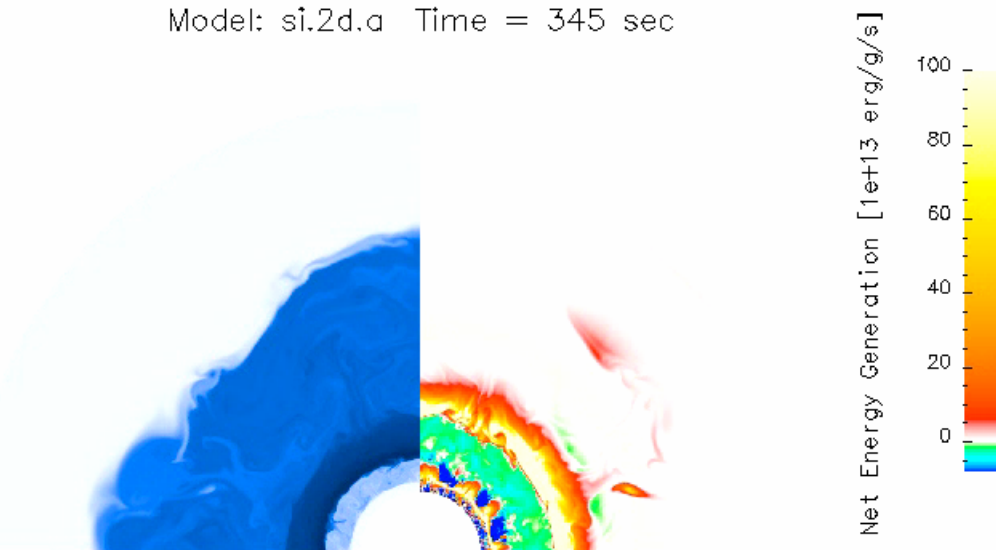
^{28}Si mass fraction energy generation



Iron Core
↓
Silicon Burning
Oxygen Burning

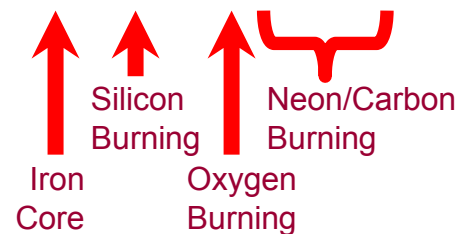


Model: si.2d.a Time = 345 sec



Net Energy Generation [10^{13} erg/g/s]

Casey Meakin & David Arnett (2006) – Steward Observatory



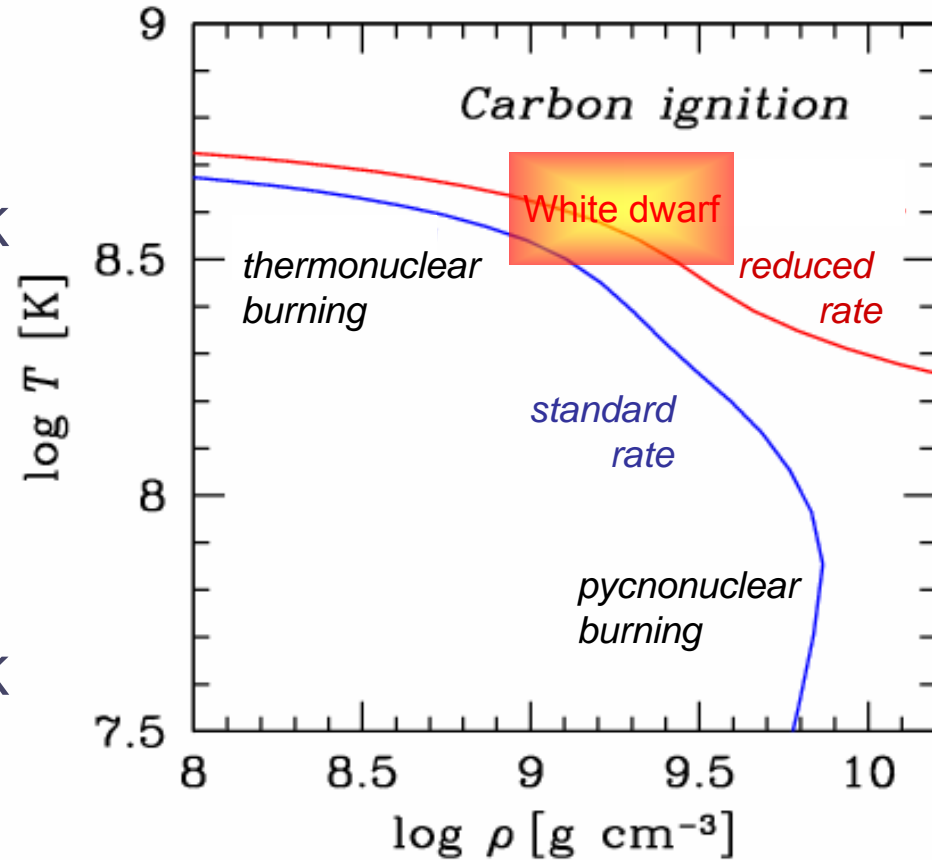
Consequences for type I SN ignition



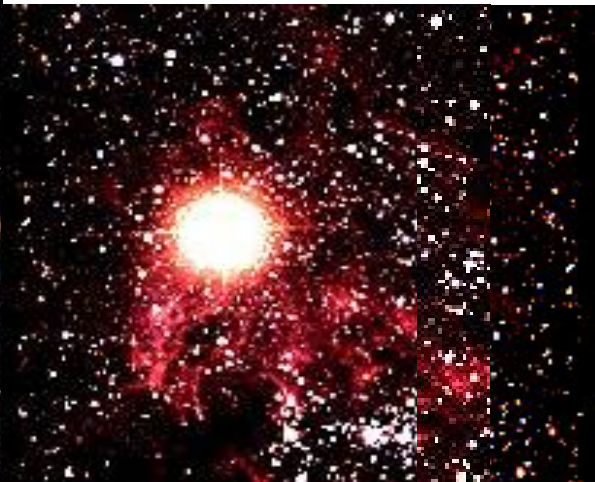
ignition conditions in white dwarfs based on the $^{12}\text{C}+^{12}\text{C}$ “standard” rate are:
 $\rho \approx 2 \cdot 10^9 \text{ g/cm}^3$ and $T \approx 3 \cdot 10^8 \text{ K}$

Reduction in rate reduces energy production ϵ_{nuc}

\Rightarrow higher temperature and/or density for ignition:
 $\rho \approx 2 \cdot 10^9 \text{ g/cm}^3$ and $T \approx 4 \cdot 10^8 \text{ K}$



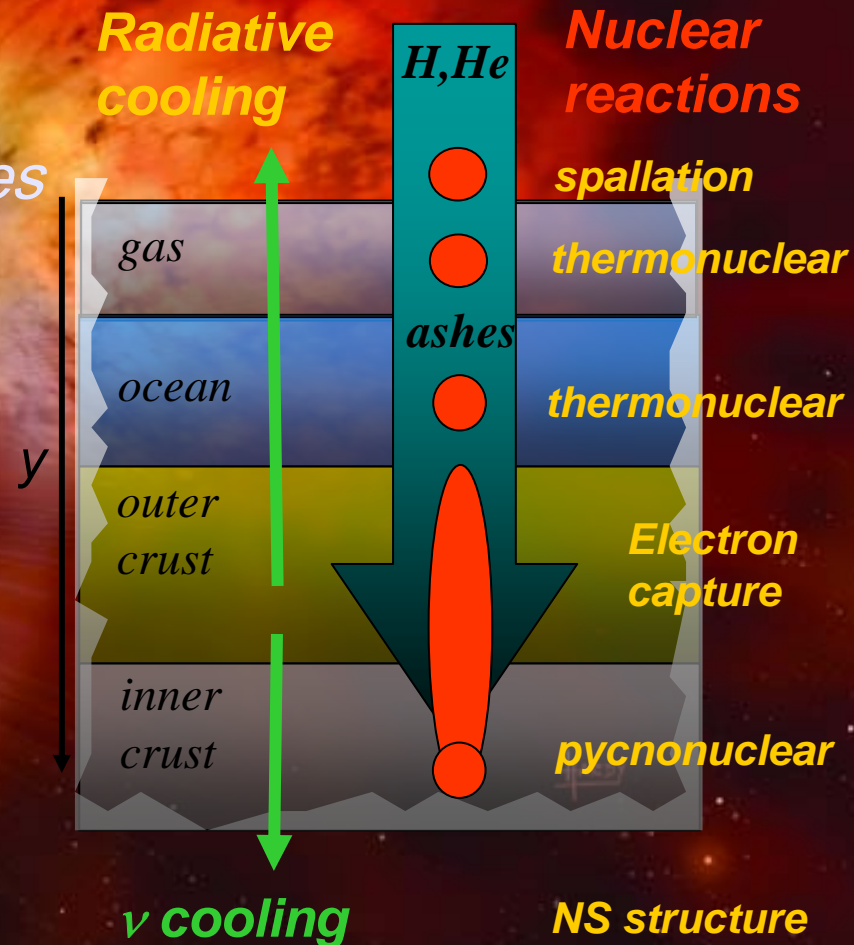
More realistic model simulations required!



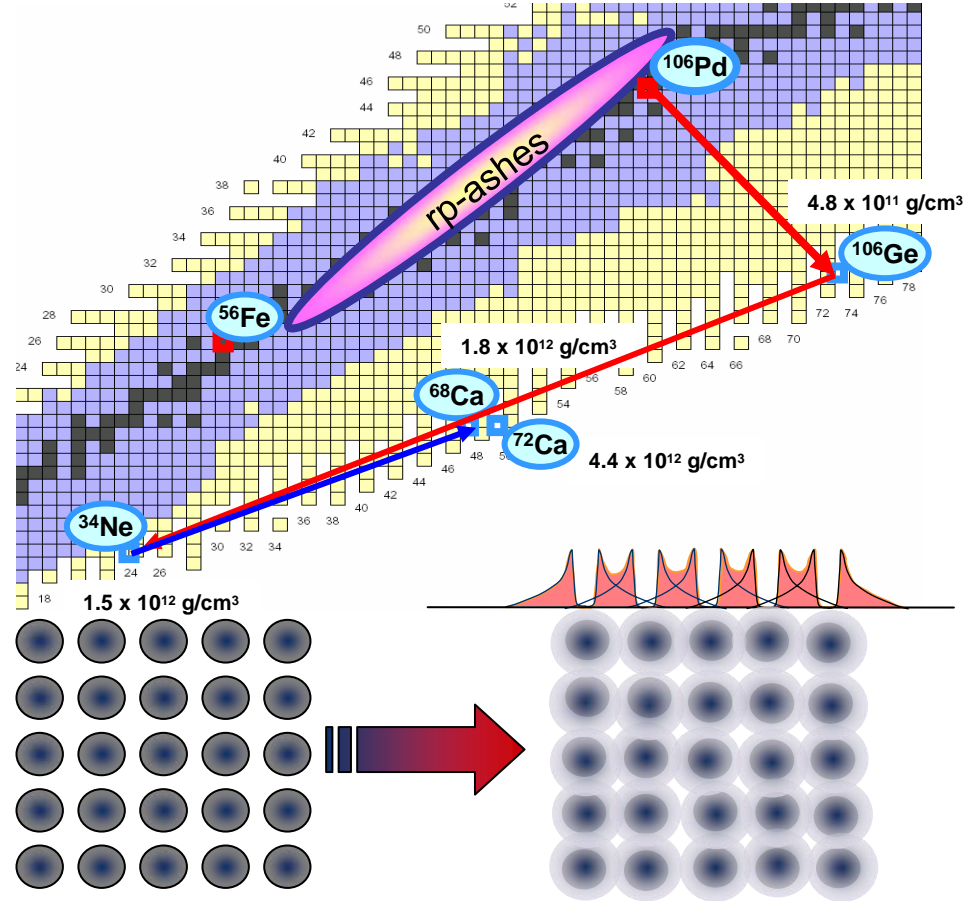
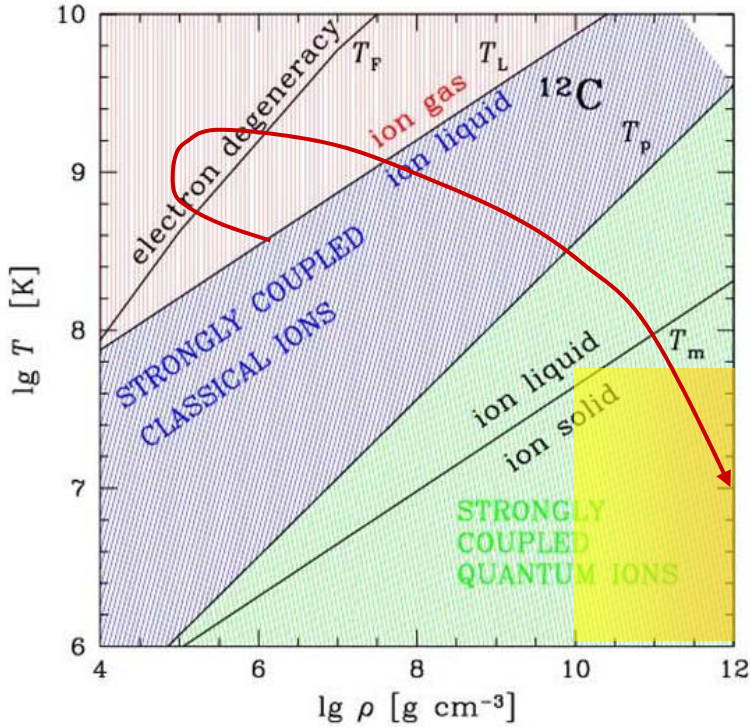
Accretion induced Reactions

Nuclear fuel feeding into a hot & dense stellar environment

⇒ ignition conditions as function of energy production & energy loss rates



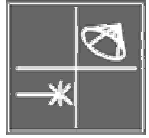
Pycnonuclear Burning



$$R_{\text{pycno}} = \left(\frac{\rho}{A} \right) \cdot A^2 \cdot Z^4 \cdot S \text{ [MeV} \cdot \text{b]} \cdot 4.76 \cdot 10^{46} \cdot \lambda^{7/4} \cdot e^{-2.52/\sqrt{\lambda}} \text{ [s}^{-1} \text{cm}^{-3}]$$

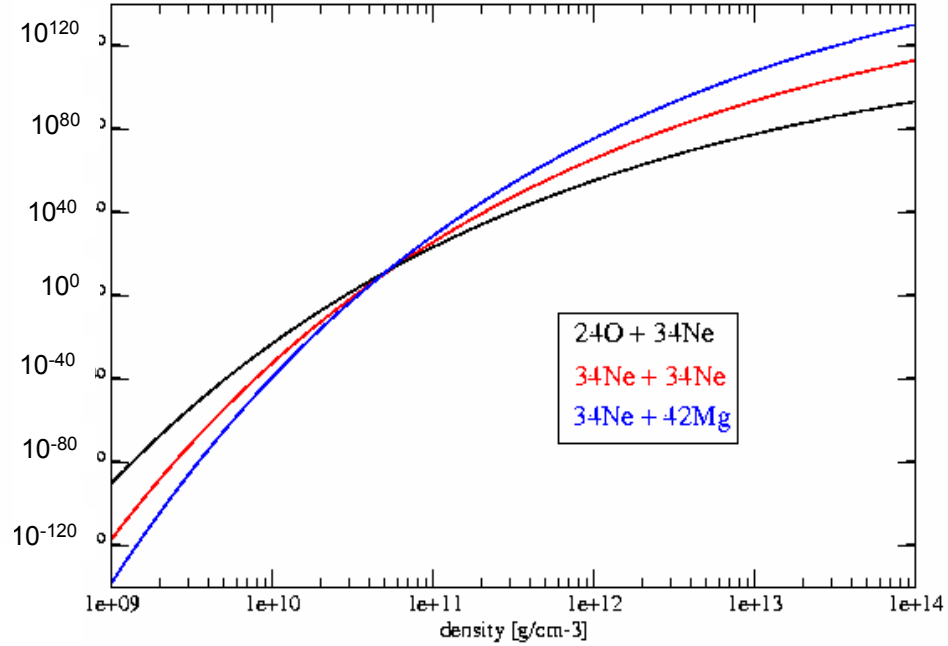
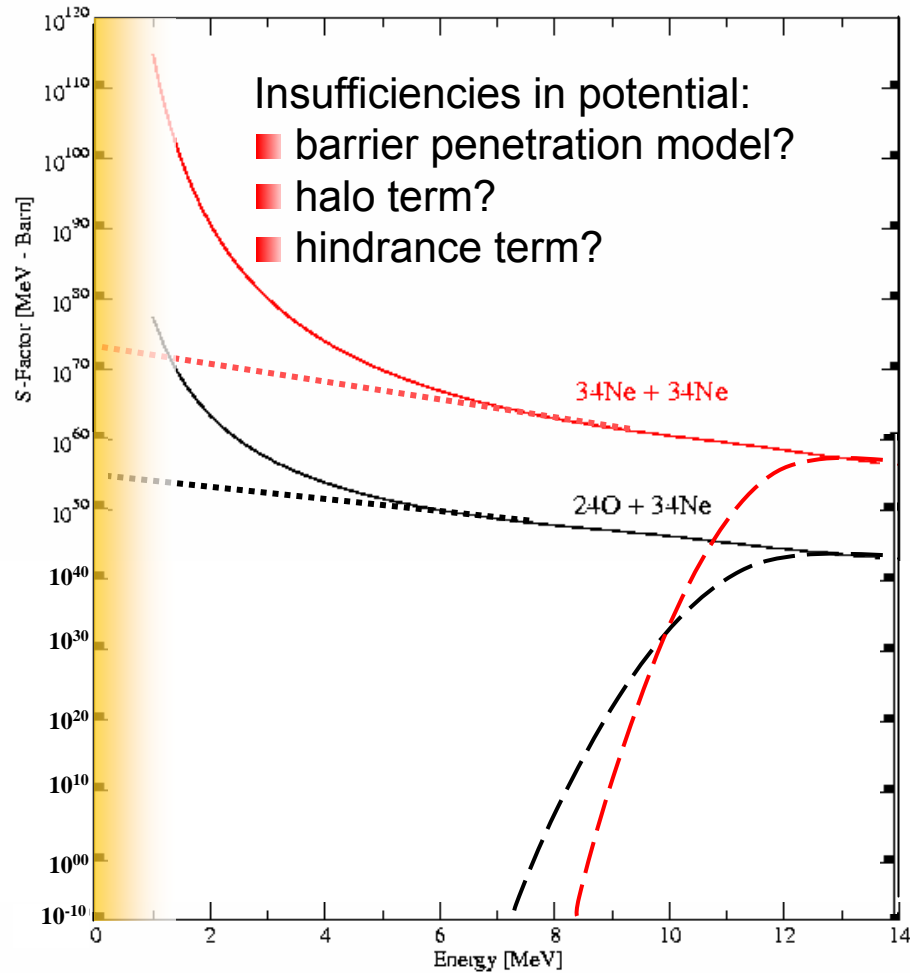
$$\lambda \equiv \text{length parameter: } \lambda = \frac{1.95 \cdot 10^{-4} \cdot \rho^{1/3}}{A^{4/3} \cdot Z^2}$$

- Cameron 1959
- Salpeter & de Haan 1969
- Schramm & Koonin 1990
- Ichimaru & Kitamura 1999
- Haensel & Zdunik 2003



J I N A

S-factor & Rate Predictions



Hindrance factor would cause a rapid reduction in the S-factor towards low T!
 ⇒ no pycnonuclear fusion burning!?

Gasques et al. PRC 2007
Neff et al. PRC 2007
Diaz-Torres et al. PL 2007